Nanolithography with diblock copolymers:
"What Fingerprints taught us about getting long range order in 2D."

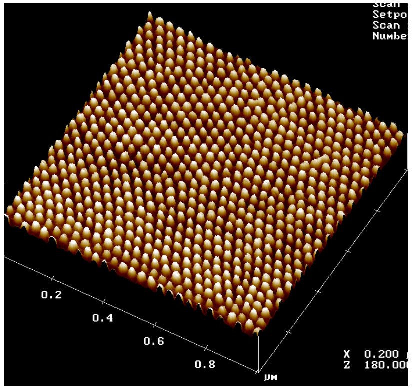

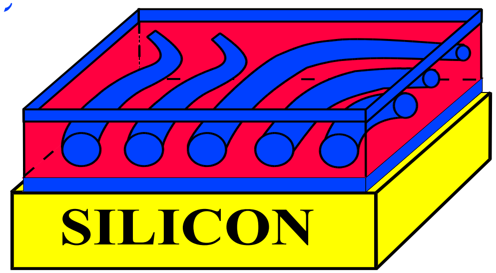

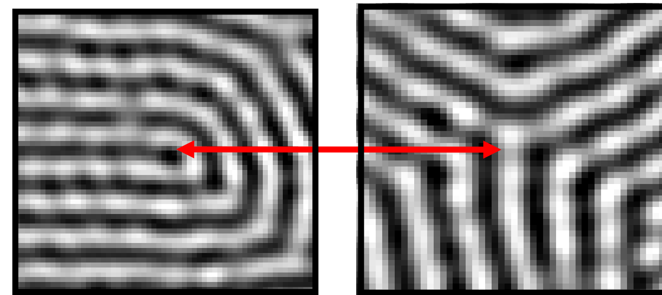

$$\vec{F} = \frac{2\rho_s k_1 k_2 \hat{r}}{|\vec{r}|}$$

Basic Idea: Massively process 5-50nm scale patterns using copolymer templates

- •How striped patterns get ordered
- •Hex Patterns
- •Completely aligned nm patterns on cm scale
- •Model for shear alignment

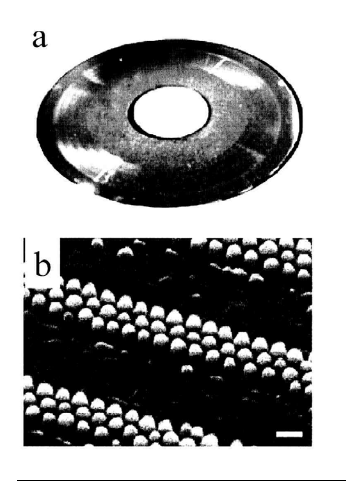

Toshiba's disk drives

Who's to Blame

Mingshaw Wu, Vincent Pelletier, Dan Angelescu, Matthew Trawick
David Huse
Princeton University, Physics Department

Judith Waller
Oxford University

Daniel Vega
ExxonMobil

Christopher Harrison
Schlumberger-Doll

Douglas Adamson
Princeton Materials Institute

PCCM-MRSEC NSF DMR-0213706; Petroleum Research Fund 35207-AC5,7

A presentation of the Chaikin-Register Polymer Lithography Group

Conventional patterning techniques in Semiconducting processing:

Feature size	
> 150nm	Photolithography
>25nm	E-Beam lithography
<25nm	?

Diblock copolymers spontaneously self-assemble into ordered structures with a scale of nanometers

→ possibility of novel patterning technique to fabricate a periodic nanoscale microstructure

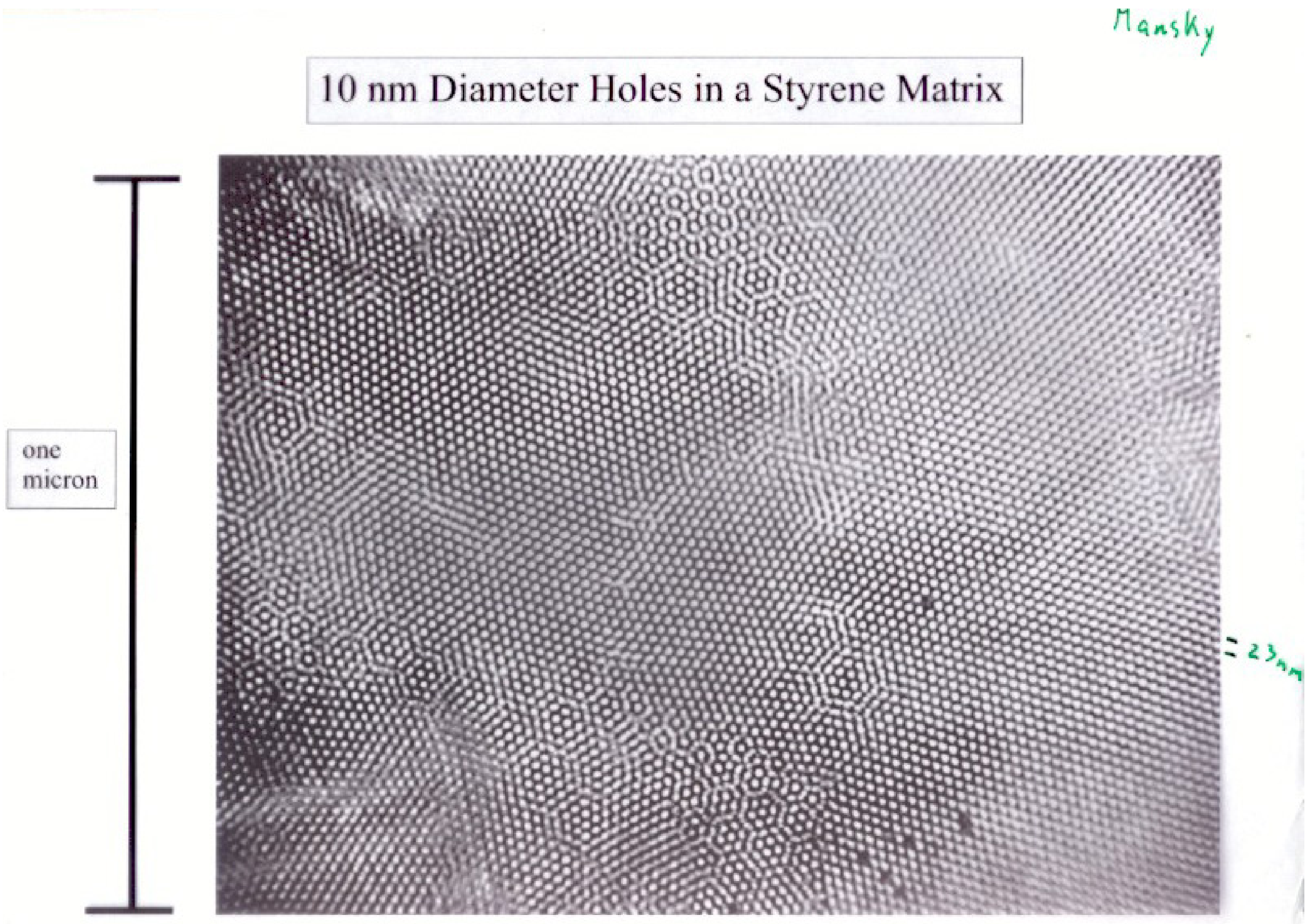

ala Lew Fetters

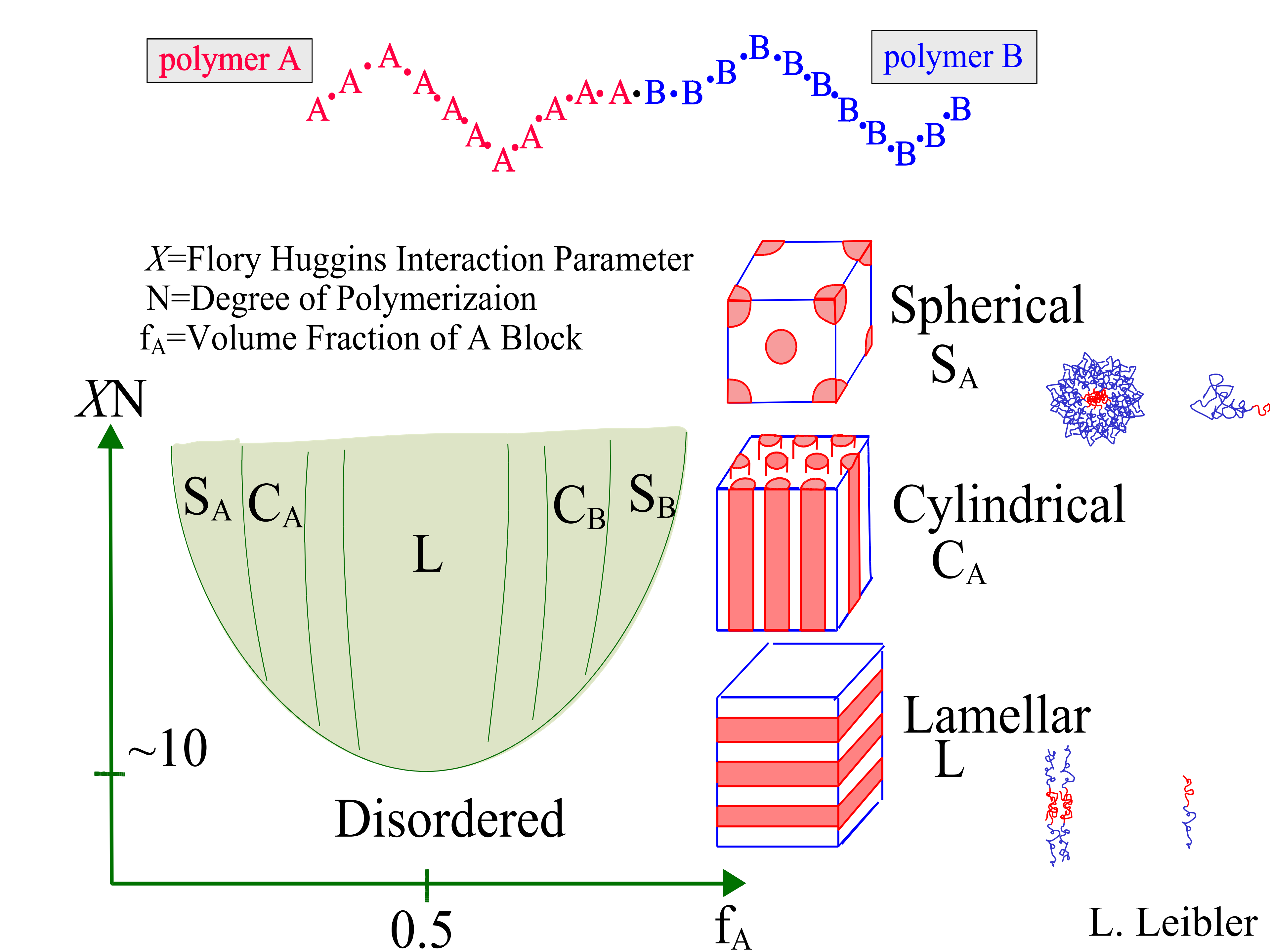
polymer A
A·A·A·A·A·A·A·A·A·A·A·A·B·B·B·B·B·B·B·B·B·B·B·B
polymer B
X=Flory Huggins Interaction Parameter
N=Degree of Polymerizaion
fA=Volume Fraction of A Block
XN
SA
CA
L
CB
SB
~10
Disordered
0.5
fA
Spherical
SA
Cylindrical
CA
Lamellar
L
L. Leibler

Diblock Copolymers

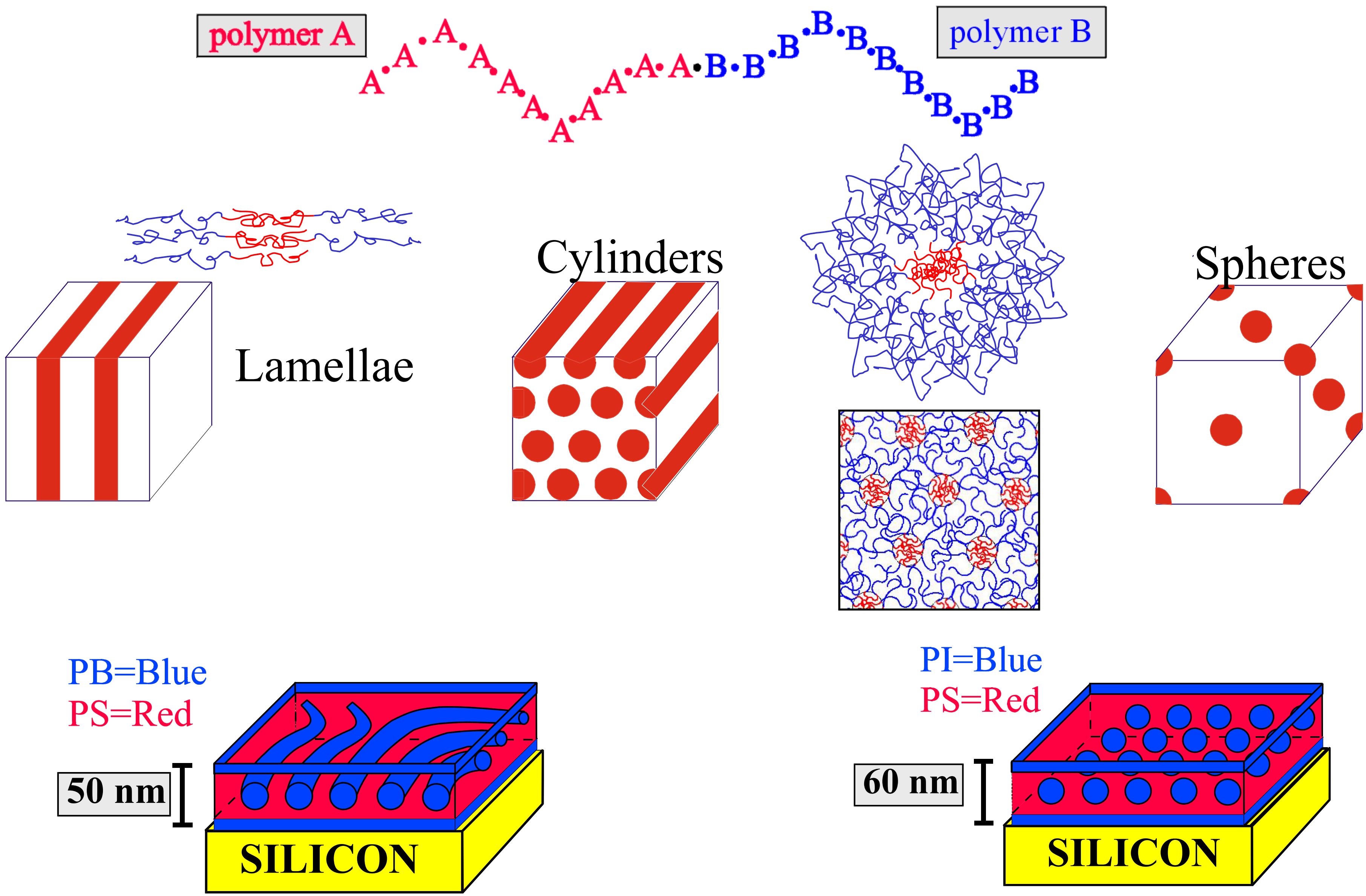

Our Diblocks are usually a plastic and a rubber

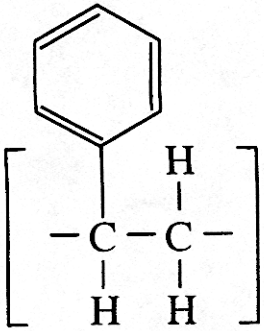

poly(styrene)

Plastic

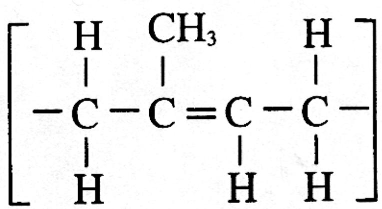

1,4 poly(isoprene)

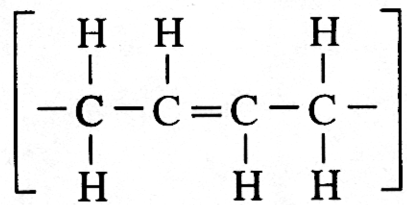

1,4 poly(butadiene)

Rubbers

e.g.

- polystyrene-polyisoprene

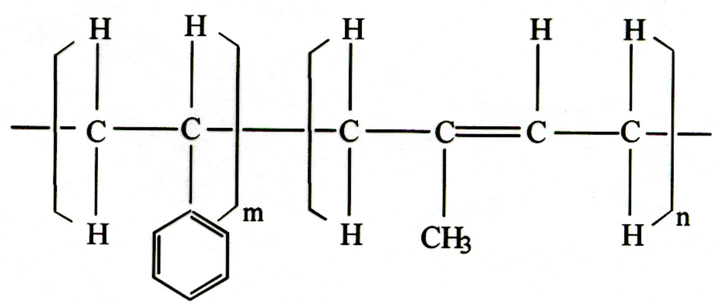

PS PI

collaboration with R.R. Li, P.D. Dapkus, and M.E. Thompson (USC)

- use MOCVD to selectively grow GaAs dots on substrate, through holes in removable "mask"

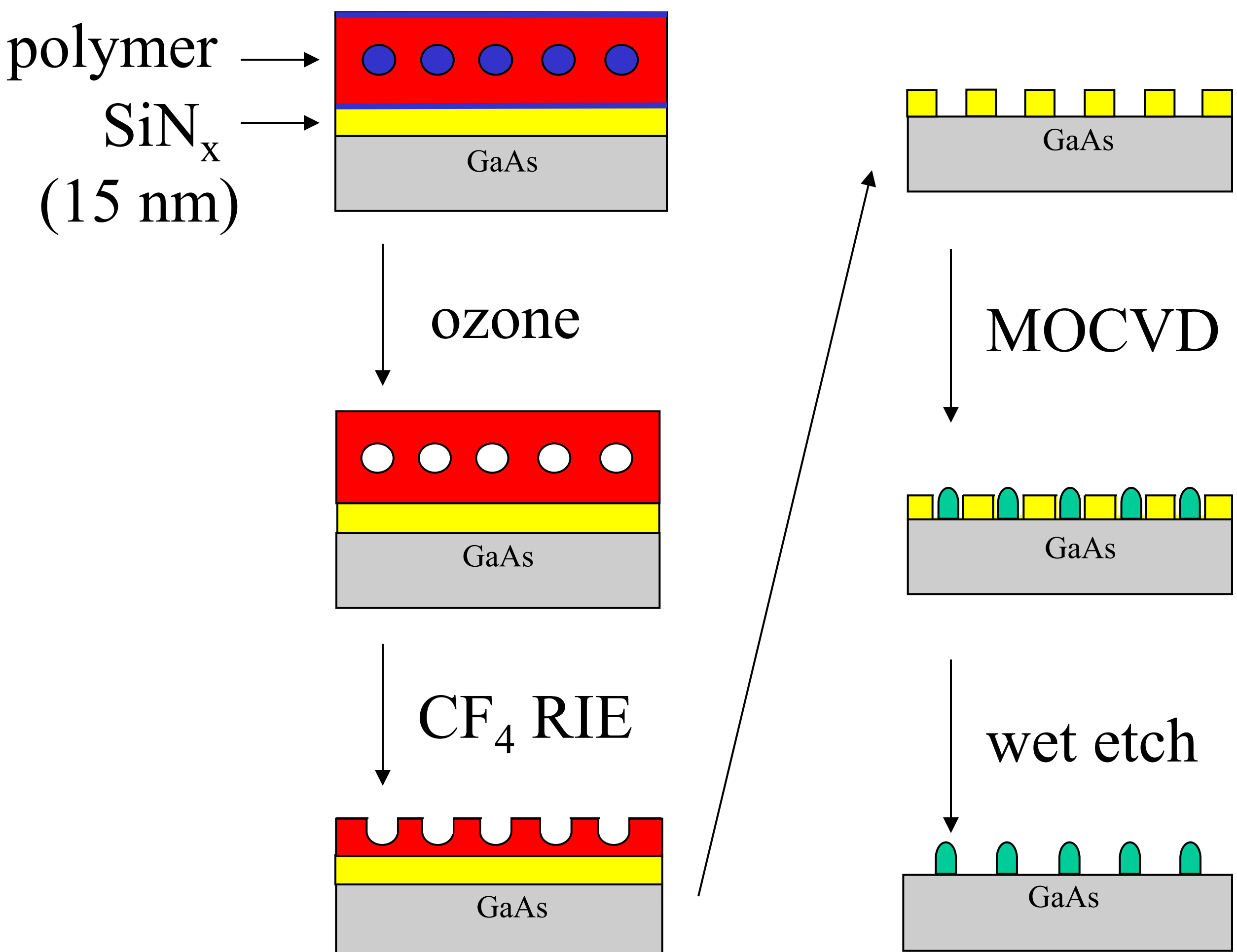

GaAs Dots Have Narrow Size Distribution

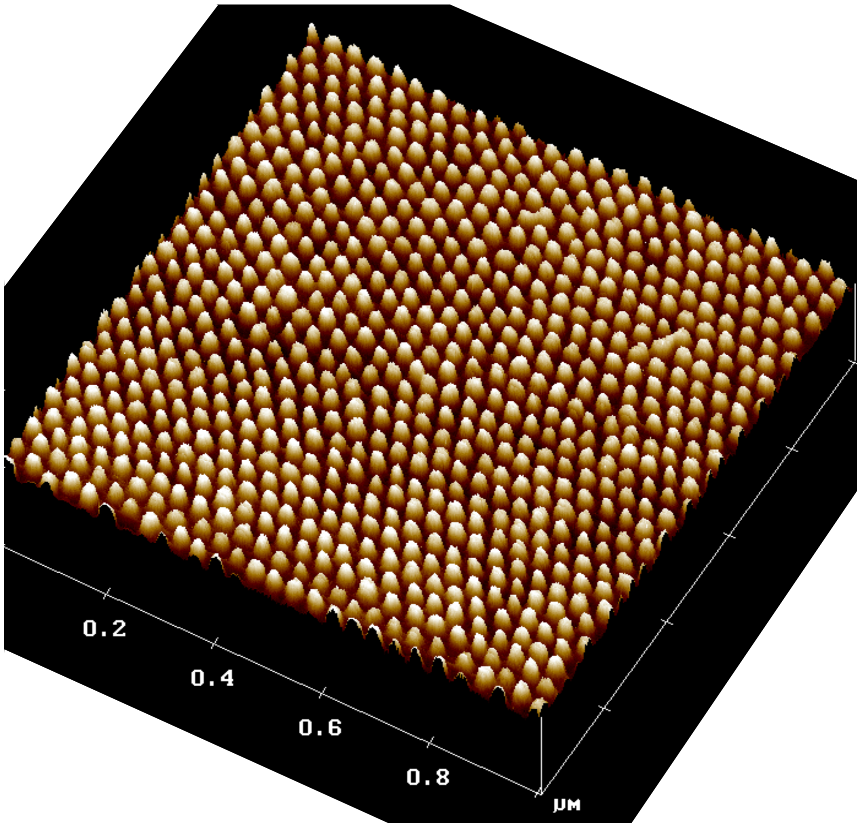

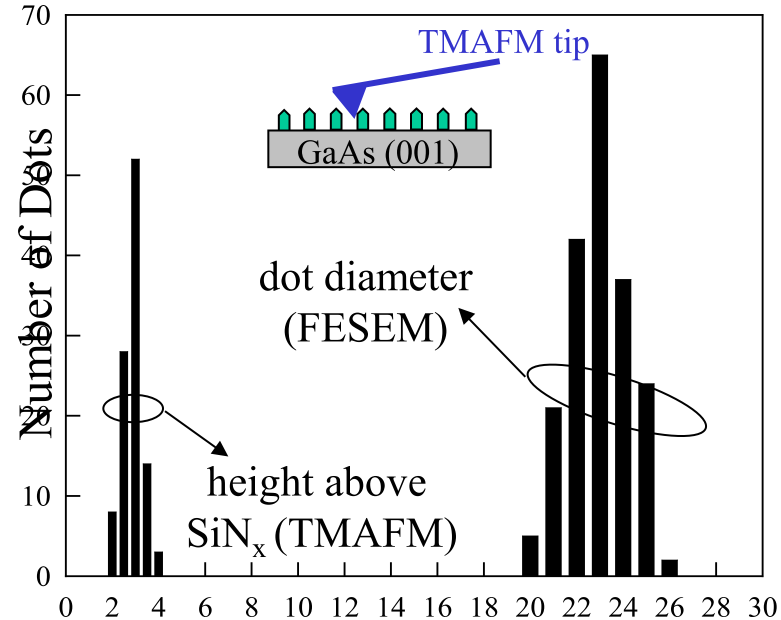

tapping-mode atomic force microscopy (TMAFM)

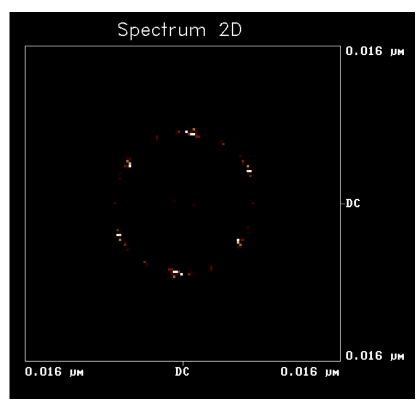

diameter:
23 ± 3 nm

overall height:
14 ± 2 nm

Kinetics of annealing from quench

Annealing of stripes – Orientational correlation length

Harrison

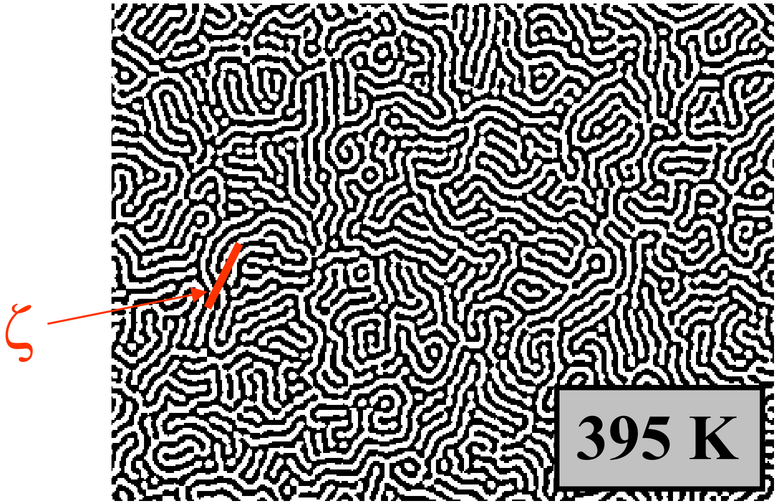

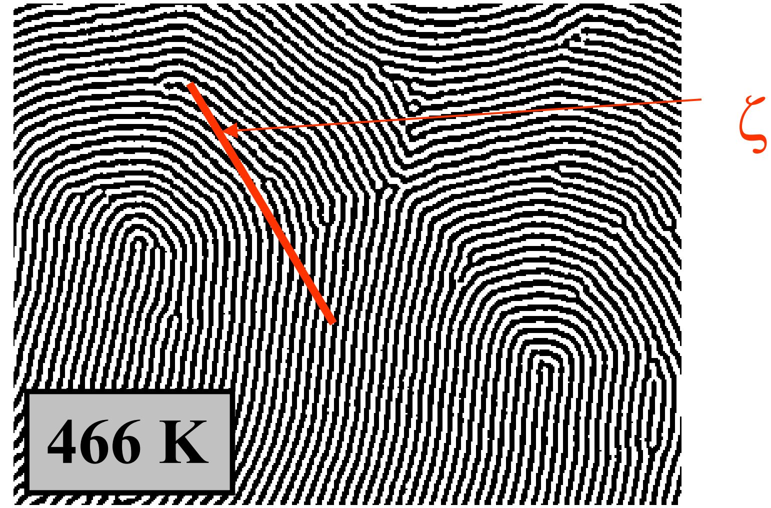

$$g_2(r) = \left\langle e^{2i\theta(\vec{r})} e^{-2i\theta(\vec{0})} \right\rangle$$

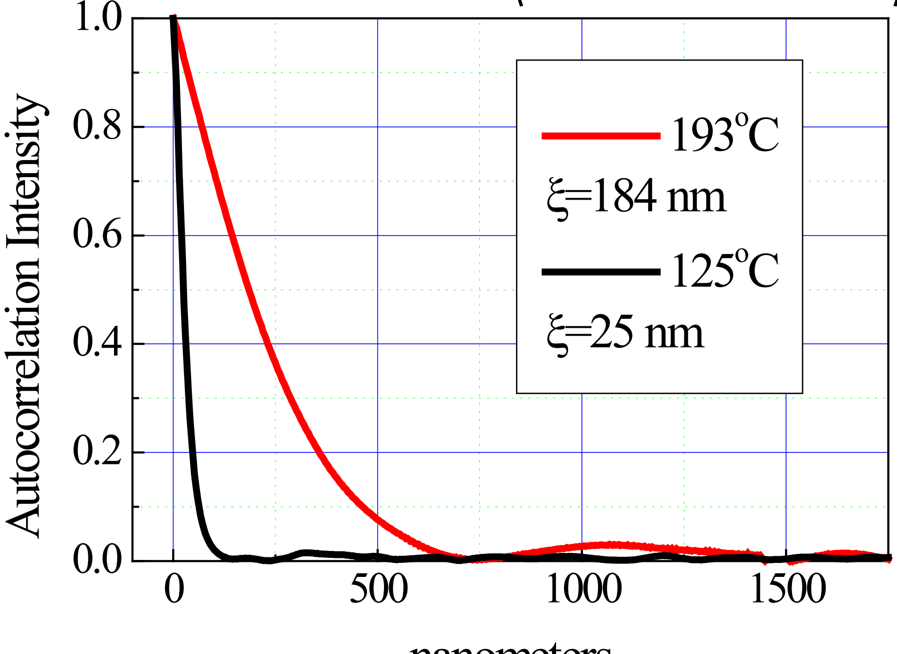

Orientational Correlation length

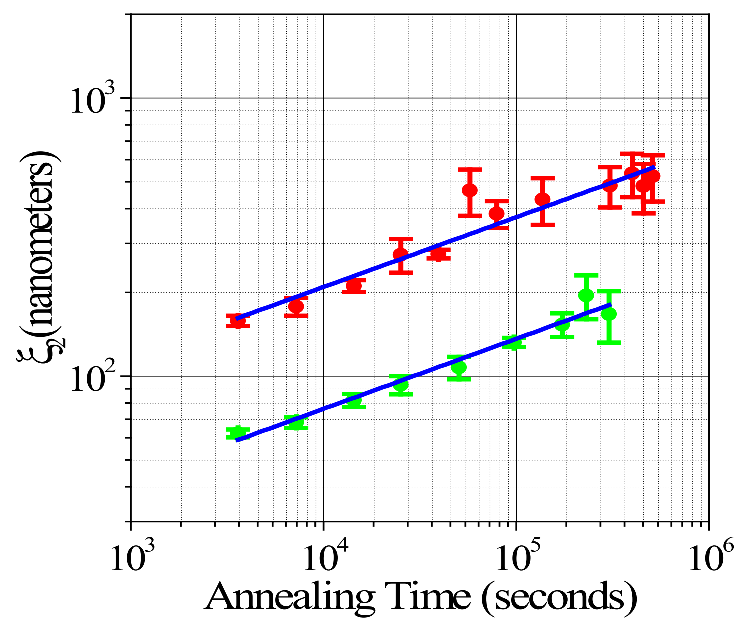

Fingerprint Identification

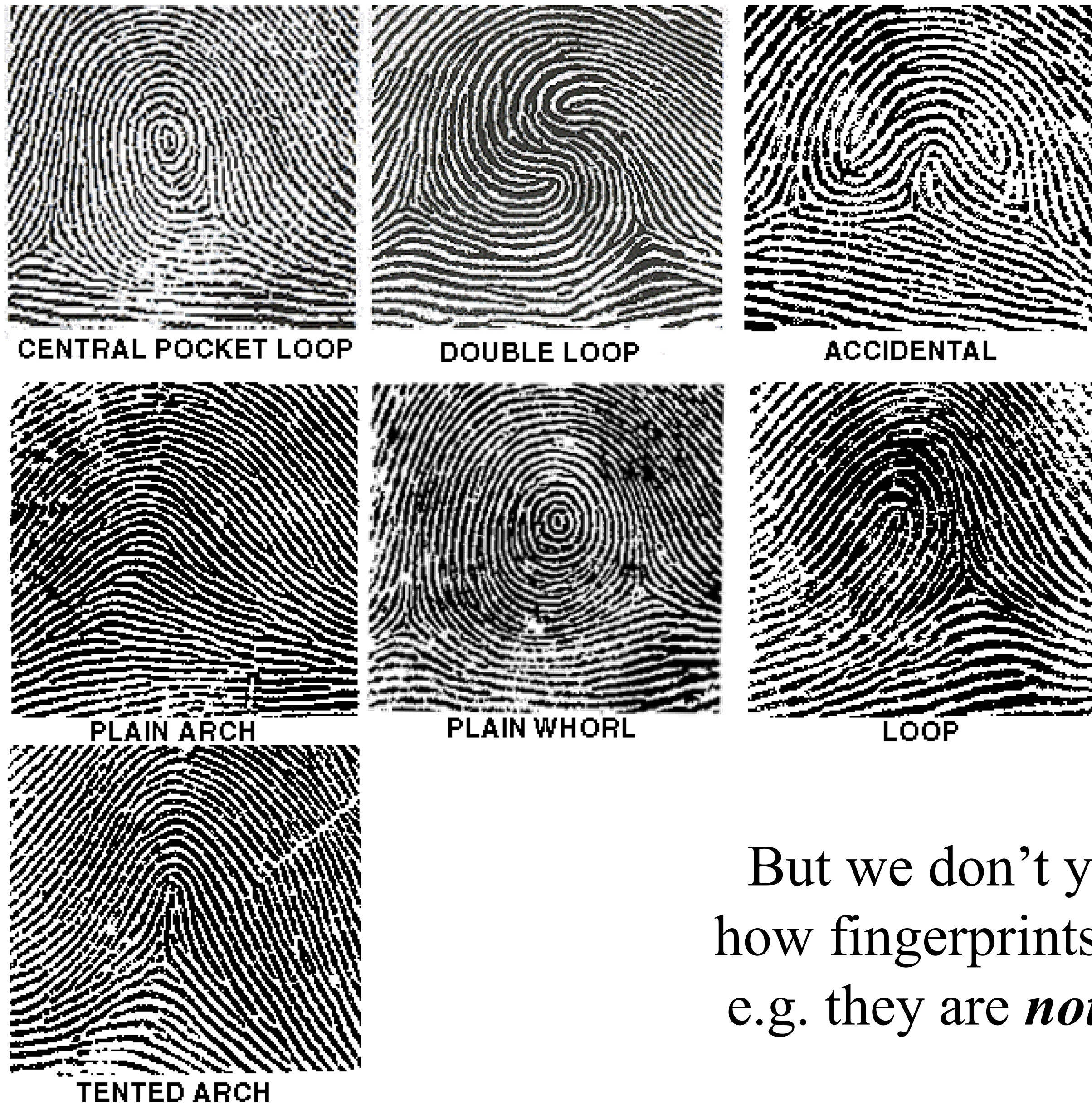

But we don’t yet know how fingerprints develop, e.g. they are ***not*** genetic.

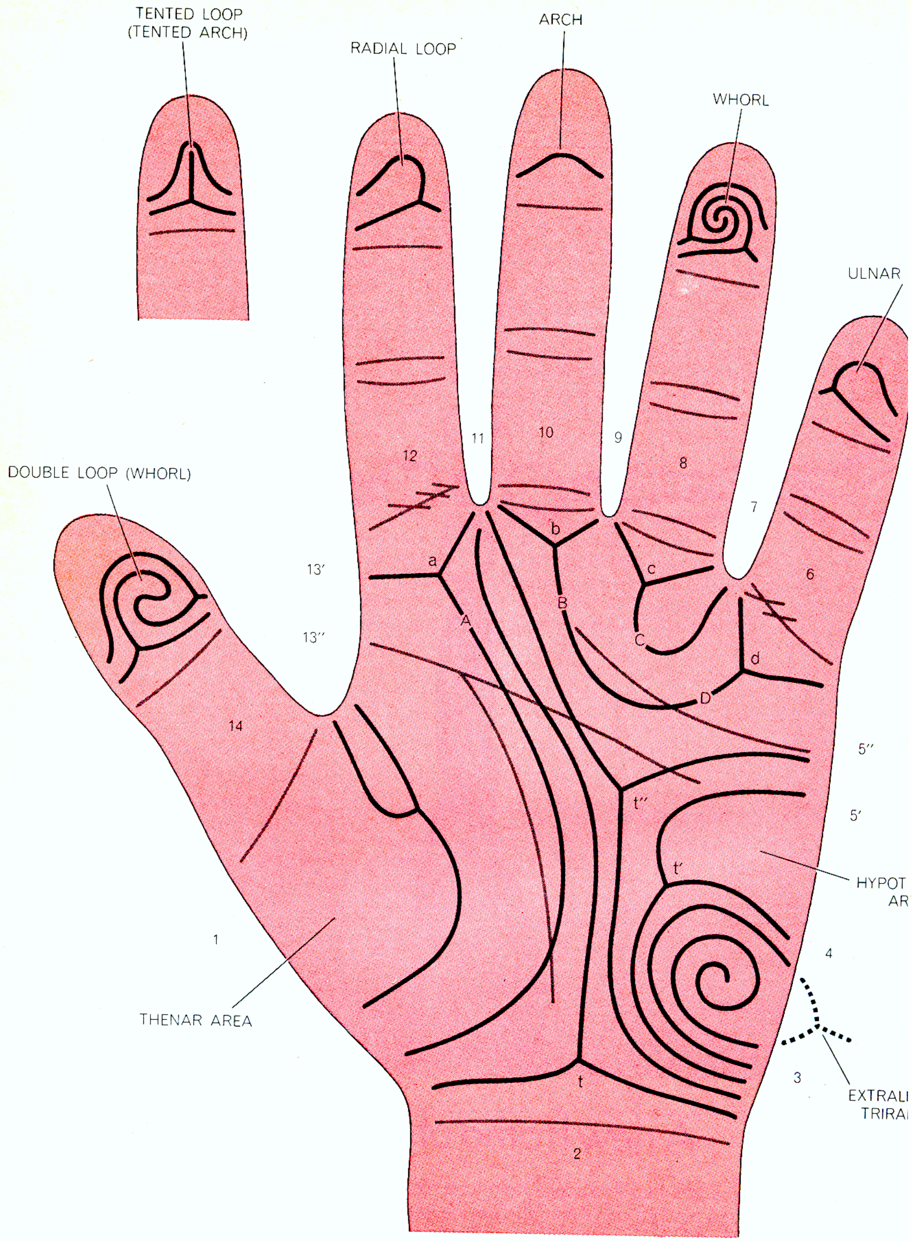

DIAGRAM OF HAND demonstrates the types and names of patterns of the ridged skin on the hands and feet. A definition of the patterns is achieved by tracing the three spokes of a triradius, which is formed where three fields of parallel ridges meet, and continuing them to the outer edges of the ridging. A number of such tracings have been made in heavy lines on this palm; the thinner gray lines are skin creases. The main lines *A*, *B*, *C* and spokes of the triradii *a*, *b*, *c* and *d*, and their exits are indic the numbers *1*, *6*, *7* and *10* respectively. The triradii labeled *t''* are called axial; they lie approximately on the axis of the digit. A number of basic patterns, such as whorls and loc identified on the fingers by their customary dermatoglyphic

DERMATOGLYPHICS

Fingerprints and the similar ridges on the palm of the hand and the sole of the foot have more uses than identification: they are also of value in anthropology, medicine and genetics

by L. S. Penrose

Every human being has a wholly distinctive set of fingerprints. Their complex patterns of parallel ridges and furrows remain unchanged throughout life and are nearly indestructible. These qualities make fingerprints an ideal means of personal identification, as Sir Francis Galton pointed out in 1890. The epidermal ridges that cover the palmar surfaces of fingertips, the palm of the hand and the sole of the foot are not, however, of interest only to the criminal investigator. Such highly personal traits can serve as valuable indexes of human variation, and they are increasingly useful in anthropology, medicine and genetics. Dermatoglyphics, as Harold Cummins of Tulane University named the study of epidermal ridges in 1926, cuts across all these disciplines.

The epidermal patterns are formed early in fetal life. At about the 12th week of gestation undulations appear on the inner surface of the epidermis. It is these undulations that later develop into a structure of ridges and furrows that contain the ducts of sweat glands, whose pores are spaced along the surface of the ridges [*see bottom illustration on next page*]. The structure increases in size as the infant grows, but the pattern is preserved unchanged; fingerprints have been shown to remain unaltered for intervals of more than 70 years. Provided that the lowest part of the epidermis is not destroyed, the pattern regenerates even after serious injury to the skin. The horny outer layers of the ridged skin are so tough that the pattern can be clearly seen on the fingers of Egyptian mummies preserved for more than 2,000 years.

When the prints of any two individuals are compared, innumerable differences in pattern can be observed on the fingers, palms and soles. This applies even to pairs of identical twins; the general configuration of their prints may be similar but there are variations in detail. Moreover, the prints of different fingers of the same person are all different from one another.

Strictly defined, dermatoglyphics does not include the study of the creases, wrinkles and cracks beloved of palmists, although these features have subsidiary significance in relation to some dermatoglyphic problems. The best-known peculiarity of this kind is the so-called simian crease, a transverse fold in the palm that is normally rare but occurs frequently in Down's syndrome, or mongolism. The cracks, smaller than the creases, tend to develop with age; they show up as white lines on prints. They have some scientific interest, but like the

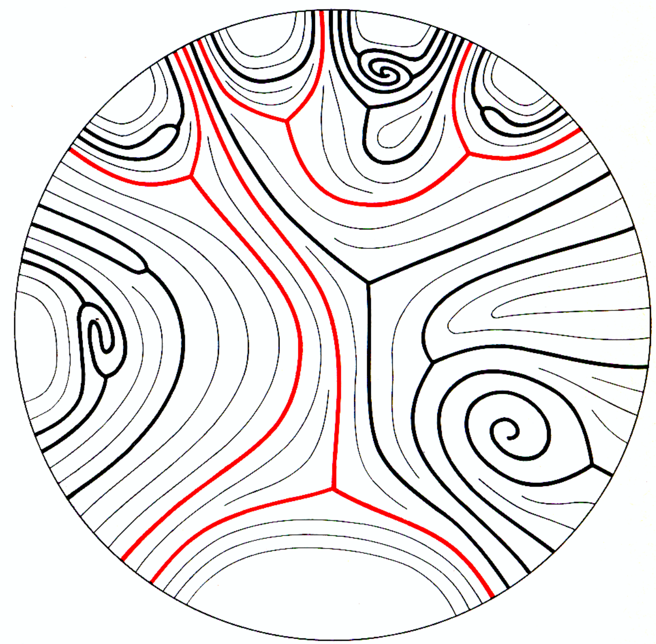

TOPOLOGICAL MAP of the hand portrayed on the opposite page shows 11 loops and 15 triradii. Removal of all loops would leave four "essential" triradii; the lines radiating from them are in color. The five small gaps represent the fingernails; the large gap represents the wrist. The ridge lines exit at right angles to the circumference except at the six gaps.

DERMATOGLYPHIC TOPOLOGY

By Prof. L. S. PENROSE, F.R.S.
Galton Laboratory, University College, London

THE ridges which form the dermatoglyphic patterns on the ventral surfaces of the hands and feet are arranged in lines which are parallel in small fields. Two kinds of discontinuity of pattern are found; these occur at the centres of what are termed loops and triradii. Around the core of a loop (Fig. 1) the direction of the ridges turns through an angle of 180°. The centre of a triradius (Fig. 2) is the point where three different fields of almost parallel ridges meet. The result produces three spokes; the angles between them are greater than 90° and are typically each 120°.

On the fingers and toes a single loop is accompanied by one triradius (see Fig. 3). When two loops are present there are two triradii, and the same applies to a symmetrical whorl in which two loops have become fused.

Fig. 1. Loop pattern

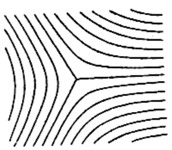

Fig. 2. Triradius

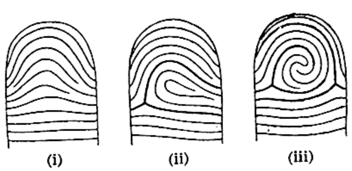

Fig. 3. Configurations on digits; (i) arch, (ii) loop, (iii) whorl

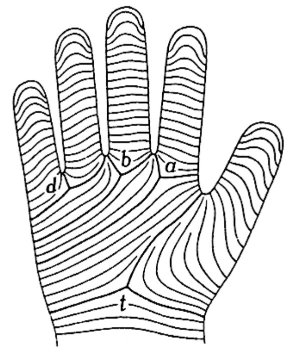

Fig. 4. Minimal number of triradii on hand

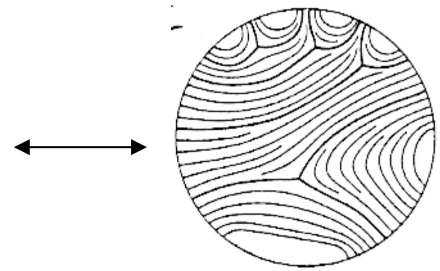

Topological equivalent

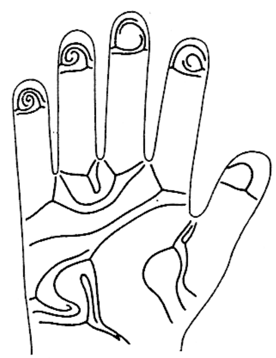

Fig. 5. Left hand with multiple ridge patterns

Curvature of the lines which is insufficient to make a loop is called an arch.

On the palms the minimal number of triradii is four. These are usually in the positions designated a, b, d and t (see Fig. 4). For every loop which occurs on the palm there is another triradius. Moreover, it can be shown empirically that, over the whole hand, including the fingers, the number of triradii exceeds the number of

For Circular area two loops are essential

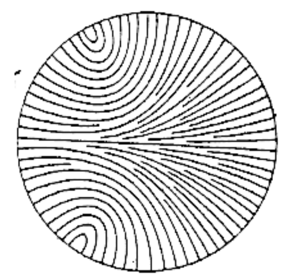

Two Loops

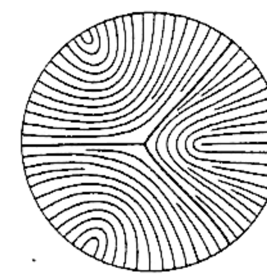

Three loops and one Triradius

$$N_{loops} - N_{triradii} = 2$$

$$N_{loops} = N_{fingers} + 1$$

$$N_{triradii} = N_{fingers} - 1$$

SH

Ann. Hum. Genet., Lond. (1979), **42**, 435
Printed in Great Britain

The topology of ridge systems

By R. PENROSE
Mathematical Institute, 24 St Giles Oxford, OX1 3LB

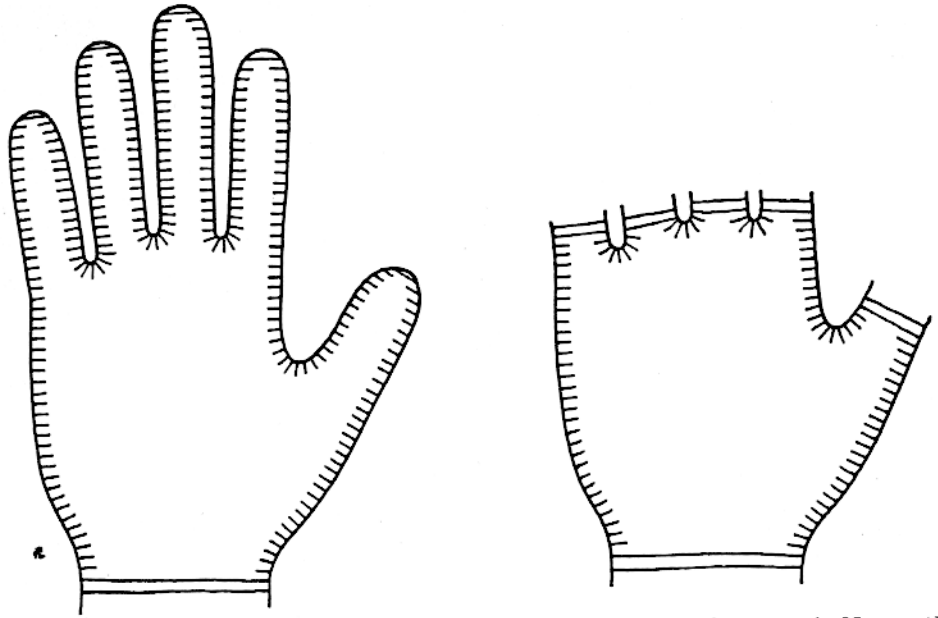

Fig. 13. The arrangement of ridge patterns around a hand or palm. The count is $N = -(D-1)$ with the number of digits being $D = 5$, here.

"The ridges are not produced by a field of force,…such a mechanism would invariably produce a directed field… and the triradius and loop would be ruled out. Instead we must expect something of a *tensor* character such as a ***stress or strain***…"

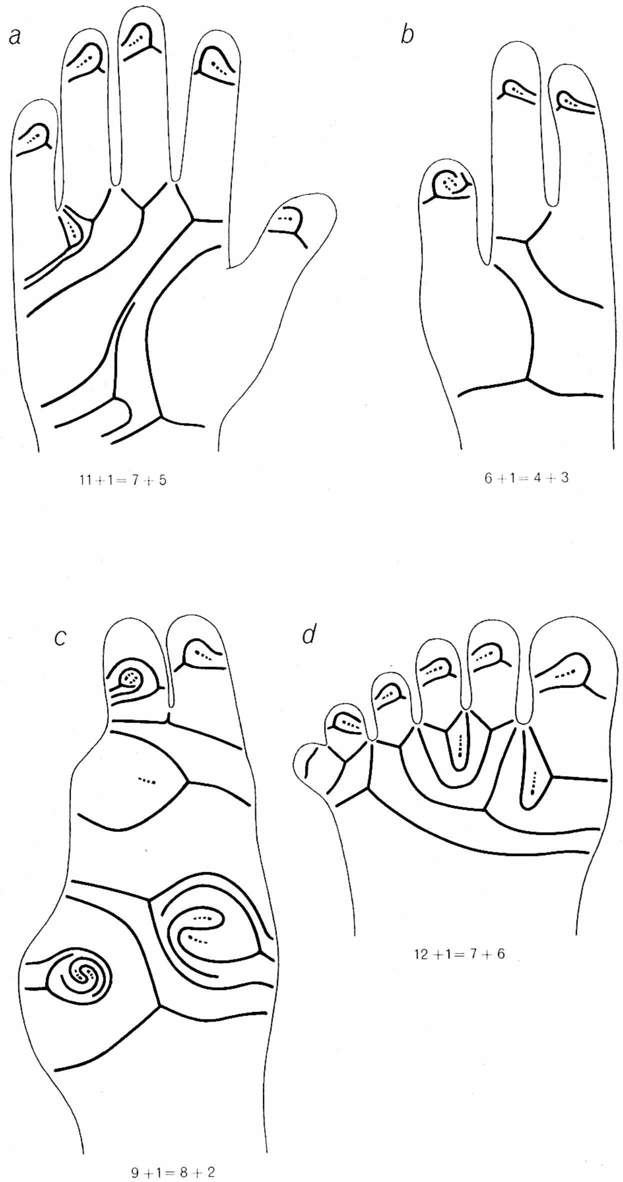

CONSISTENT RELATION appears, even in abnormal hands and feet, between the number of loops, *L*, the number of triradii, *T*, and the number of digits, *D*. It is expressed in the formula $T + 1 = L + D$ and manifested here in the normal left hand (*a*) and abnormal right hand (*b*) of the same person, in the right hand (*c*) of a patient with ectrodactyly, or congenitally absent digits, and in left foot (*d*) of a patient with a congenitally extra digit.

digits. On a normal hand or foot the number of triradii must therefore exceed the number of loops by four. Exceptions to this rule arise when the ridges for a short distance lie parallel to, instead of at right angles to, the edge. In such circumstances a triradius (or loop) that belongs to the pattern can lie just beyond the ridged surface; it is "extralimital" but must be counted in applying the formula.

The formula is useful in checking that all triradii on a palm have been recorded. It is particularly convenient in studying patterns on the sole, because triradii between the toes are frequently awkward to print and the whole configuration cannot be appreciated unless their positions can be identified. The formula applies in developmental defects in which the number of fingers or toes is altered: If there is an extra finger or toe, it is associated with an extra triradius; if digits are missing, there are fewer triradii.

Little is known about the developmental conditions that determine the orientation of epidermal ridges. The conventional view has been that the ridges represent lines of tension, and that they run at right angles to the direction of pressure in the embryonic epidermis. On the whole the lines seem to take approximately the shortest paths; if they continued from the ball of the finger, the palm or the sole onto the back surface of a limb, they would encircle the digit, the hand or the foot. Yet they are not contour lines or geodesics. An alternative suggestion for the origin of ridges, which would agree well with most of their properties, is that they follow not lines of tension but rather lines of greatest positive curvature (or of least negative curvature) in the embryonic epidermis. In the early stages of formation of the limb buds in man, the pads that form the developing palm and sole have been supposed to produce the tension required to align the ridges. On the other hand, the pads could provide curvature to which the growing skin may be sensitive. Lines of curvature on a smooth surface have a parallel arrangement; loops occur on ellipsoids and triradii occur on saddle shapes of certain kinds. The shape of the fetal human fingertip is not incompatible with what would be required if the lines of curvature were to produce a loop and a triradius, as is commonly found.

The natural variation demonstrated by epidermal ridge patterns has been studied in different populations by anthropologists and in families by geneticists. Hereditary influences have been

Annealing of stripes

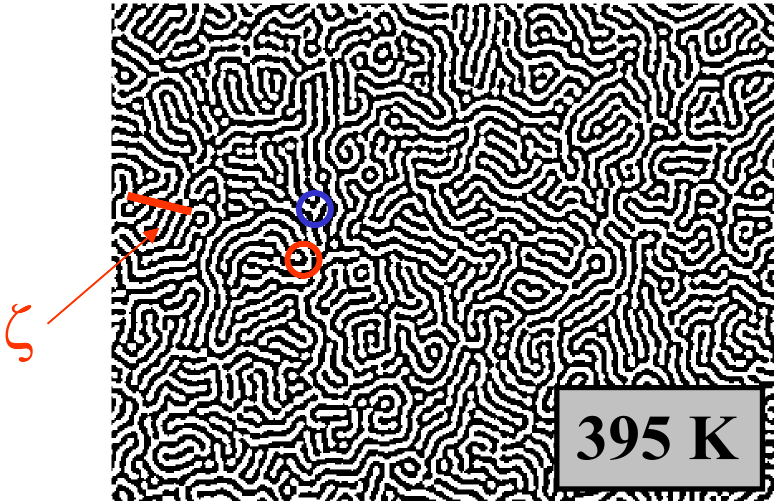

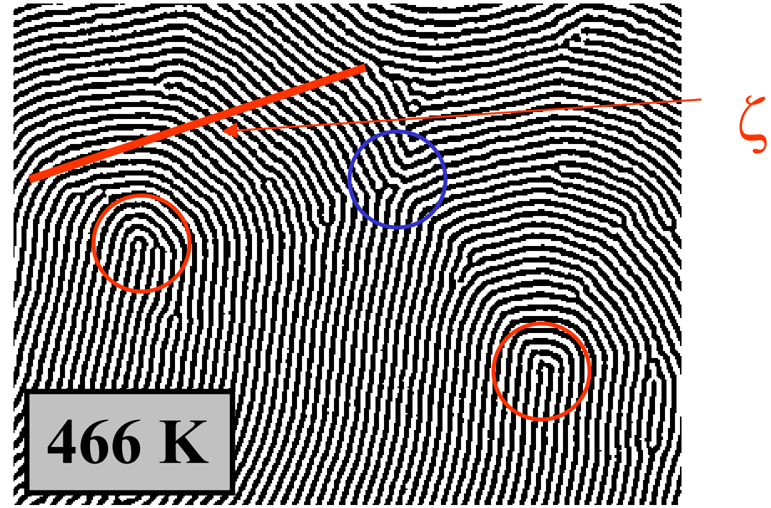

Orientational Correlation length

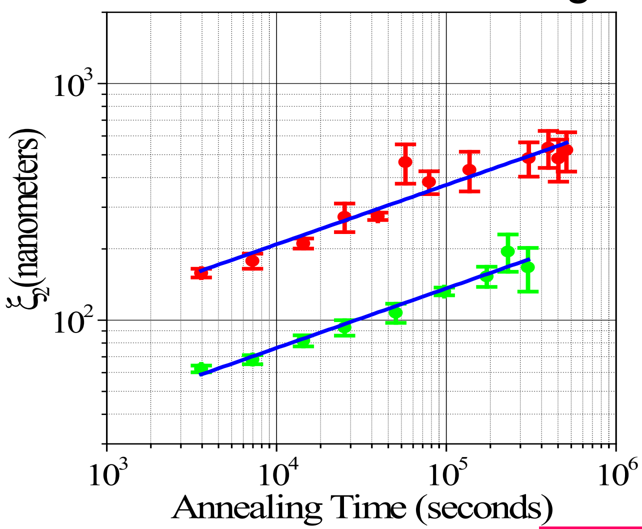

Average Distance between Disclinations

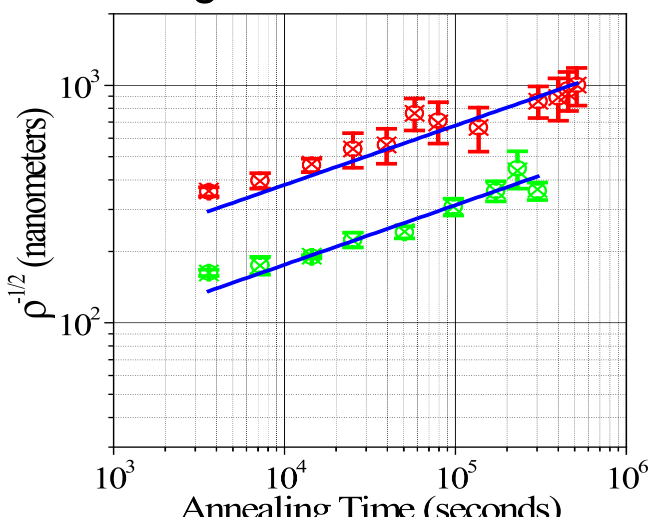

$$\zeta_2 \sim \rho^{-1/2} \propto t^{1/4}$$

Observing Pattern Coarsening

- Spin coat diblock copolymer solution to make thin film. Selecting a film thickness of one microdomain layer allows us to study a 2D system. The diblock copolymer volume fraction selects resulting morphology.
- Anneal above glass transition temperature on atomic force microscope (AFM) hot stage.
- Quench to ambient temperature for imaging with tapping mode AFM tip. Phase contrast is generated by the difference in moduli of the two blocks.

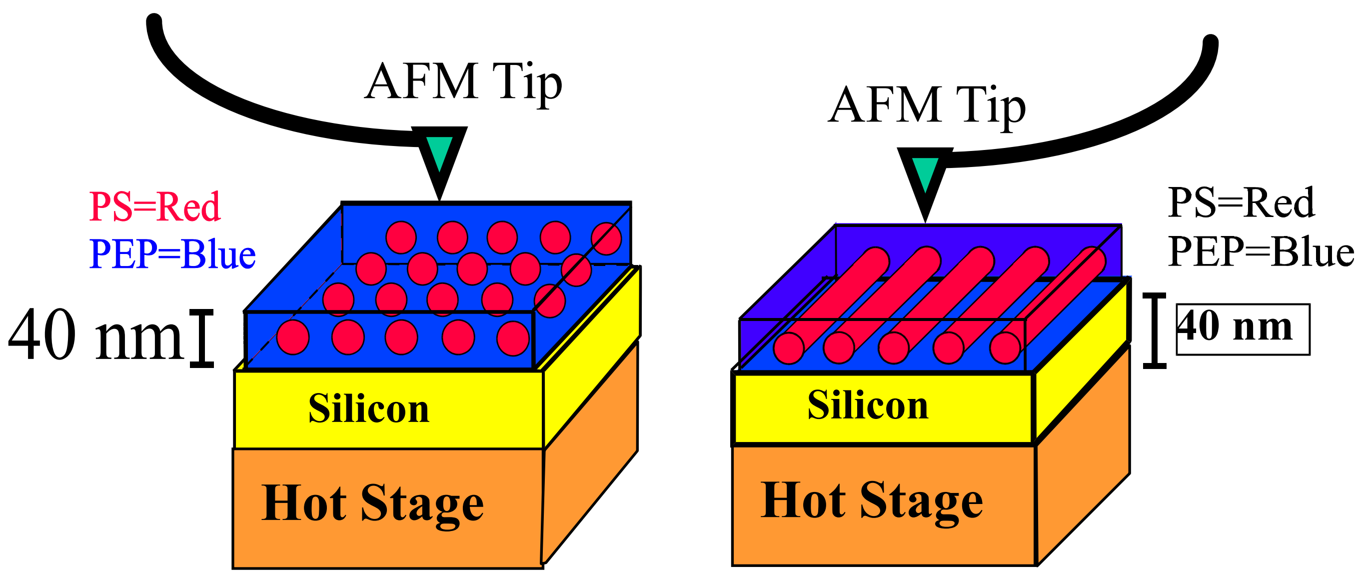

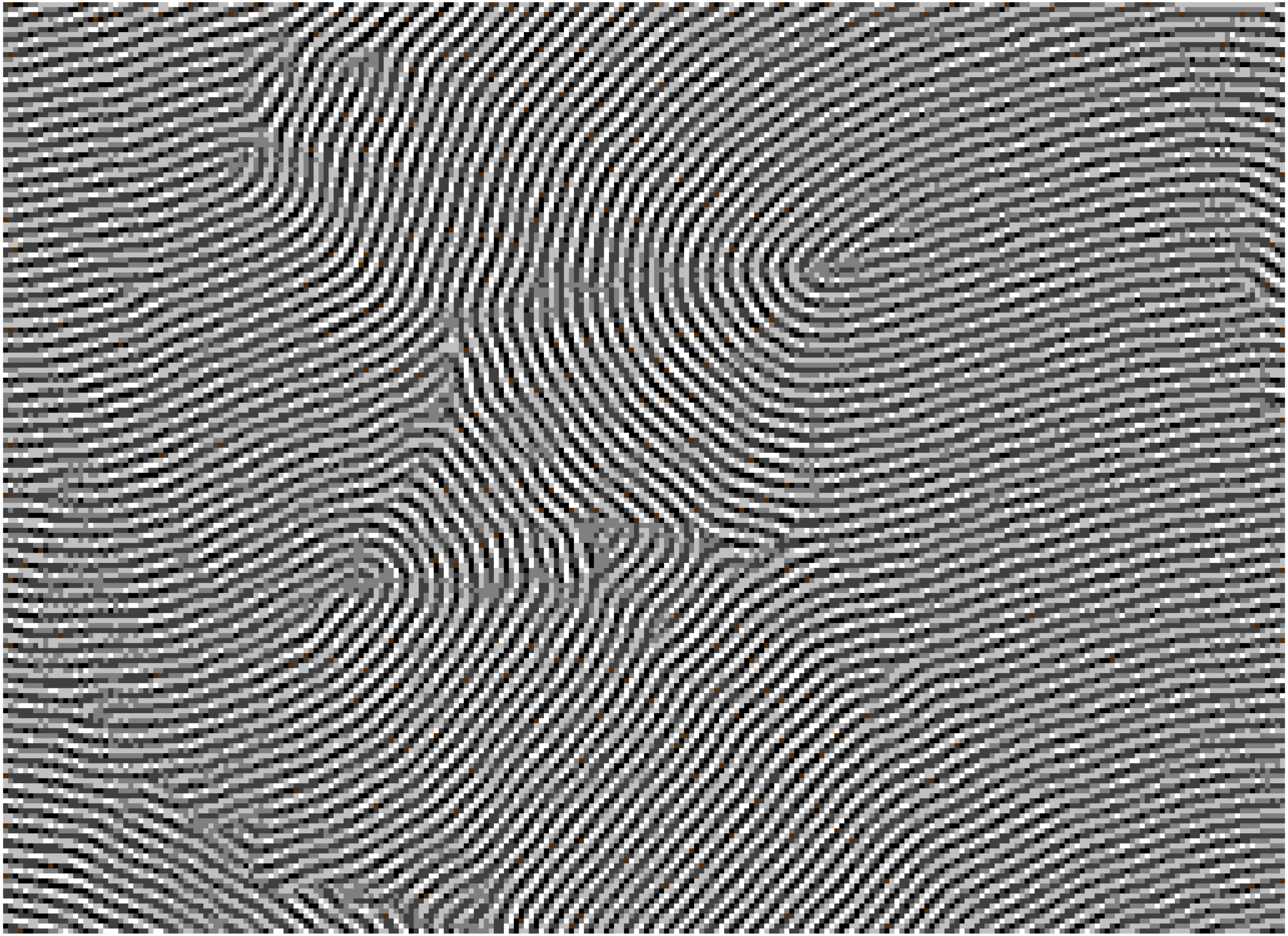

Annealing by quadrupole annihilation

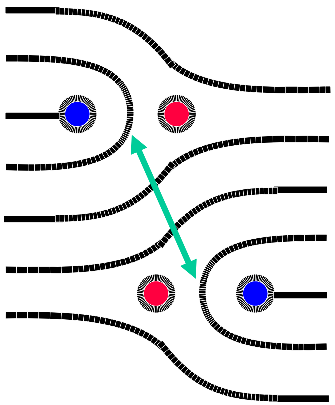

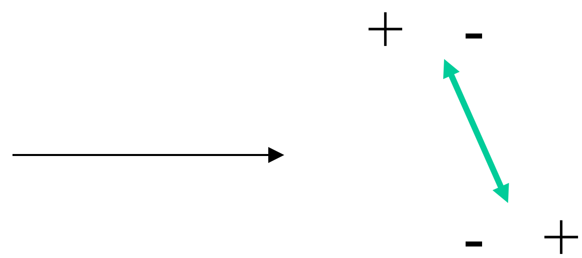

dipole-dipole

$F \sim p^2/r^3$

$$v = \mu F \sim 1/r^3$$

$$\frac{\partial r}{\partial t} \sim \frac{1}{r^3}$$

$$r^3 \partial r \sim \partial t$$

$$r^4 \sim t$$

$$r \sim t^{1/4}$$

$$\xi \sim t^{1/4}$$

Why not dipole annihilation?
For stripes moving disclination produces dislocations

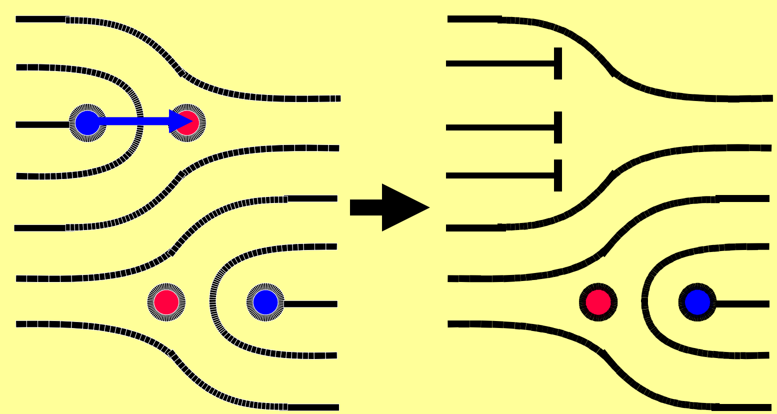

Experimental setup

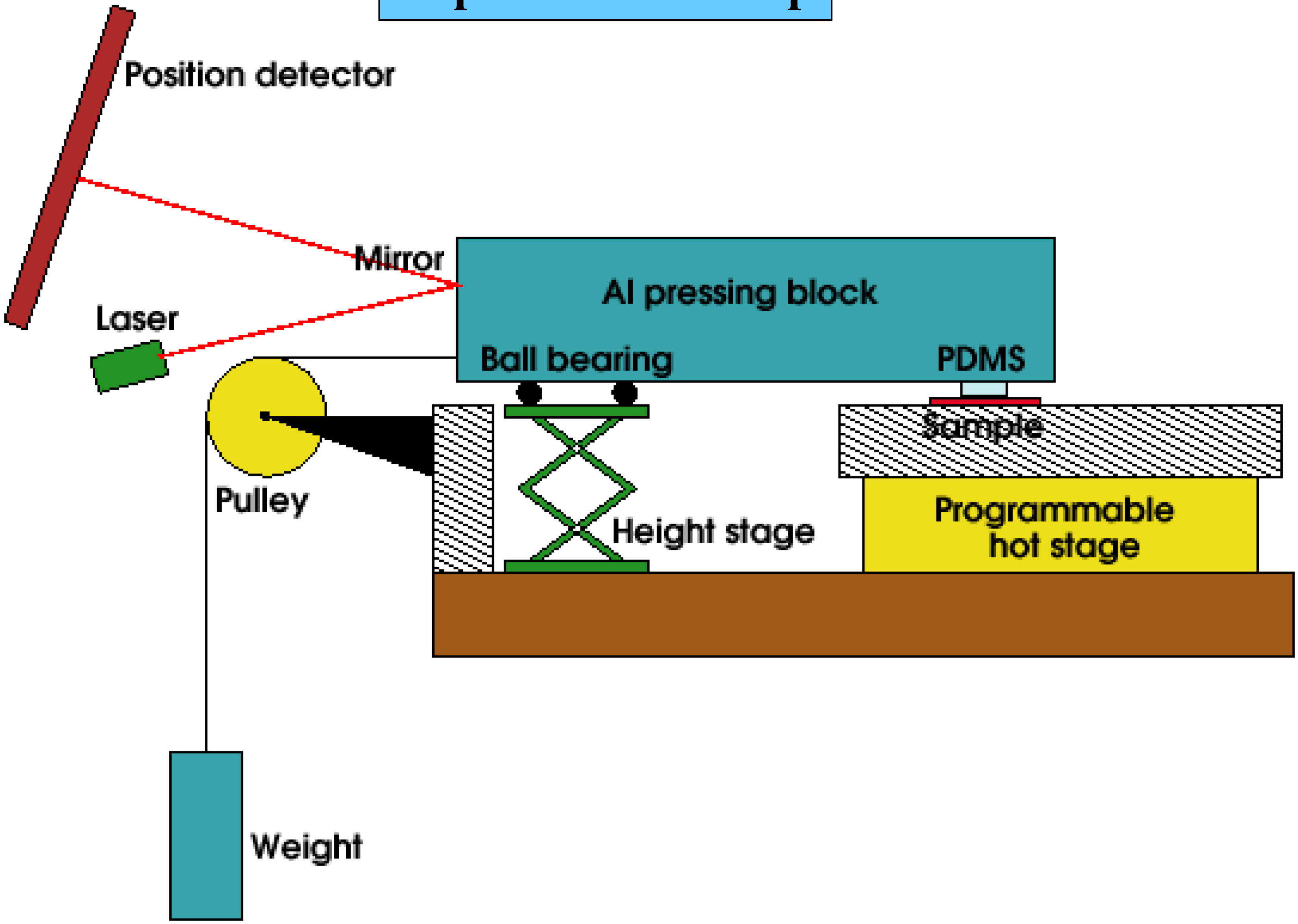

Wondershearfridge Alignment

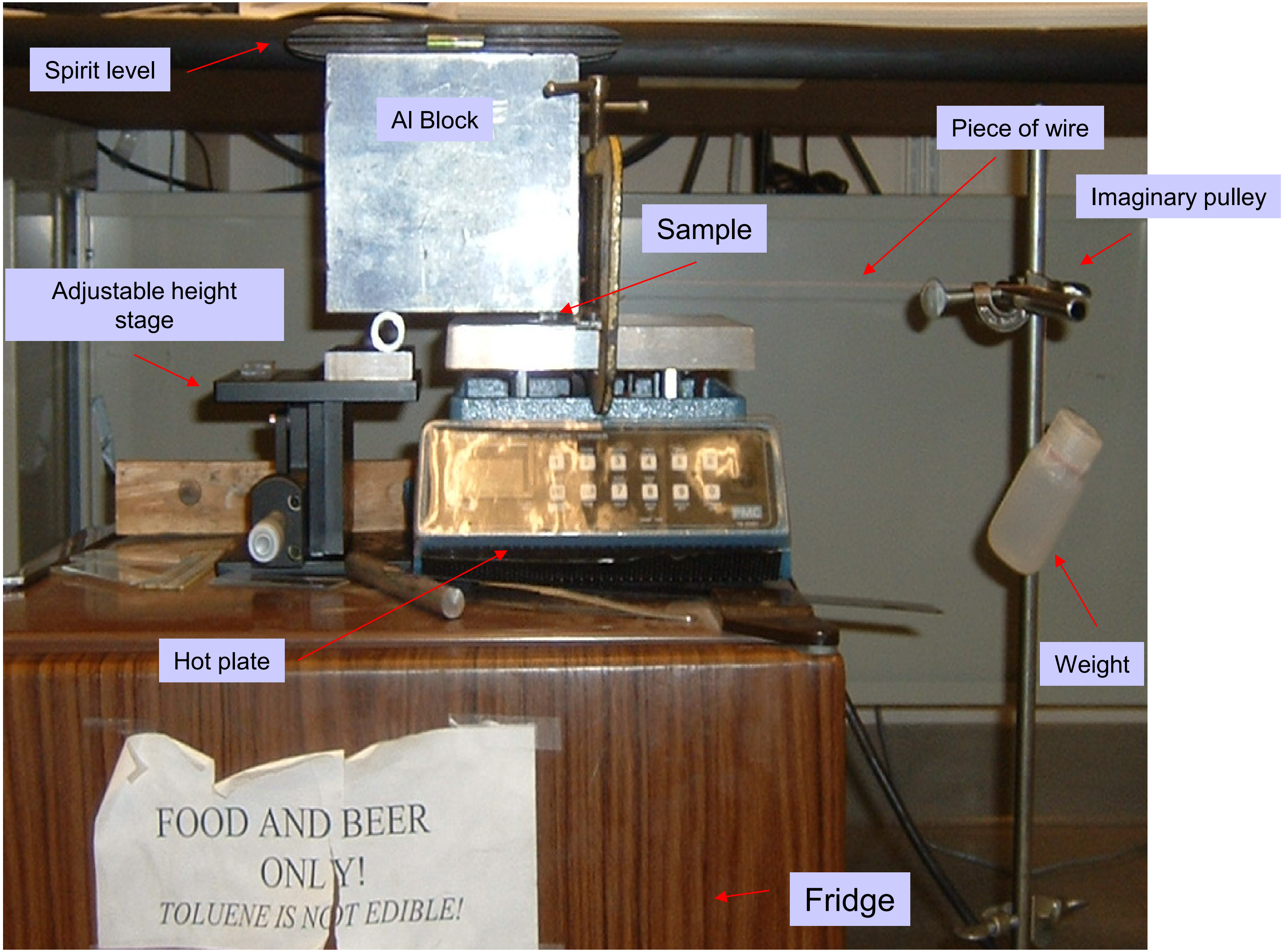

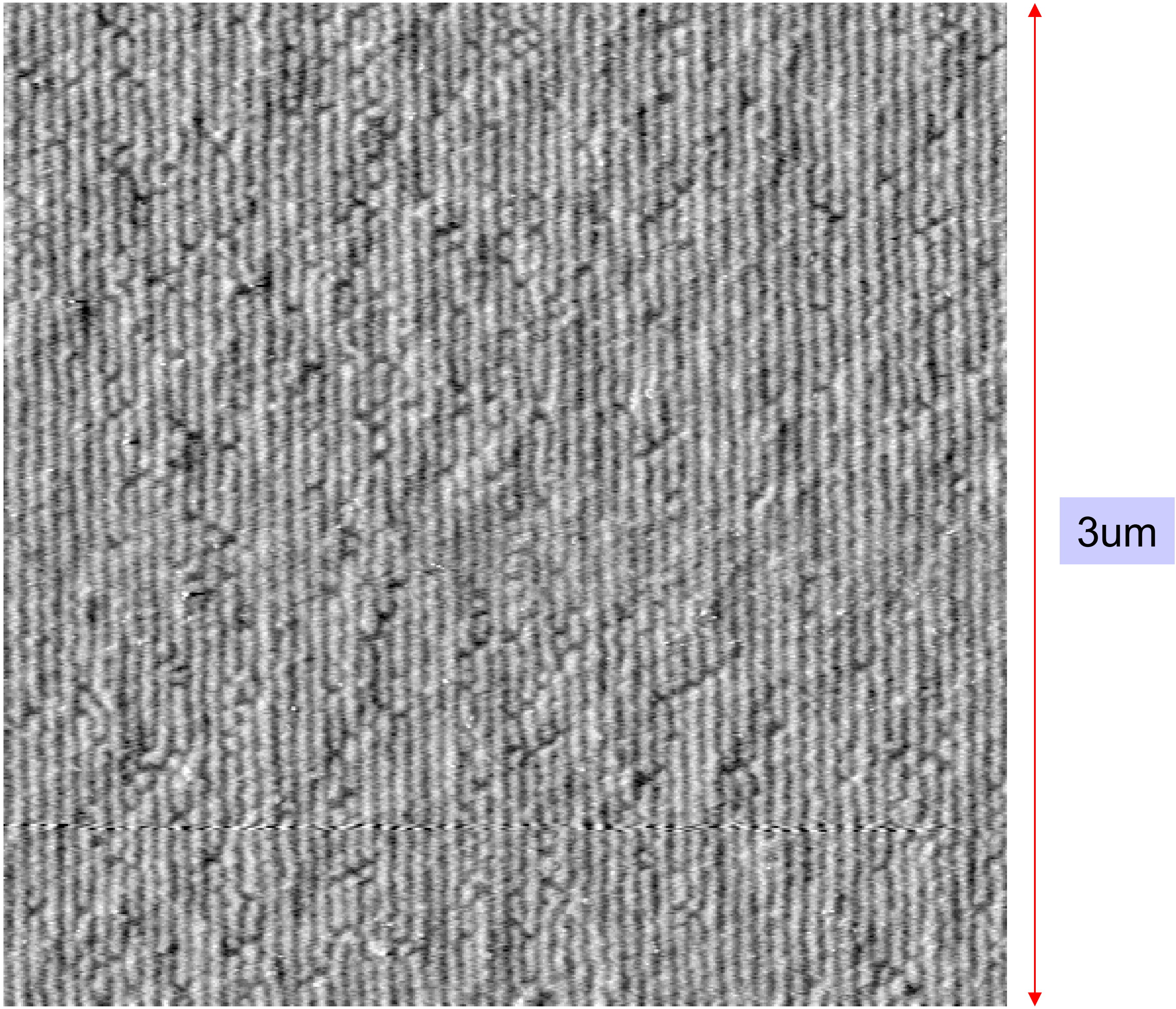

PS-PHMA 2 Hrs at 150 deg C: Alignment ☺

Angelescu & Waller

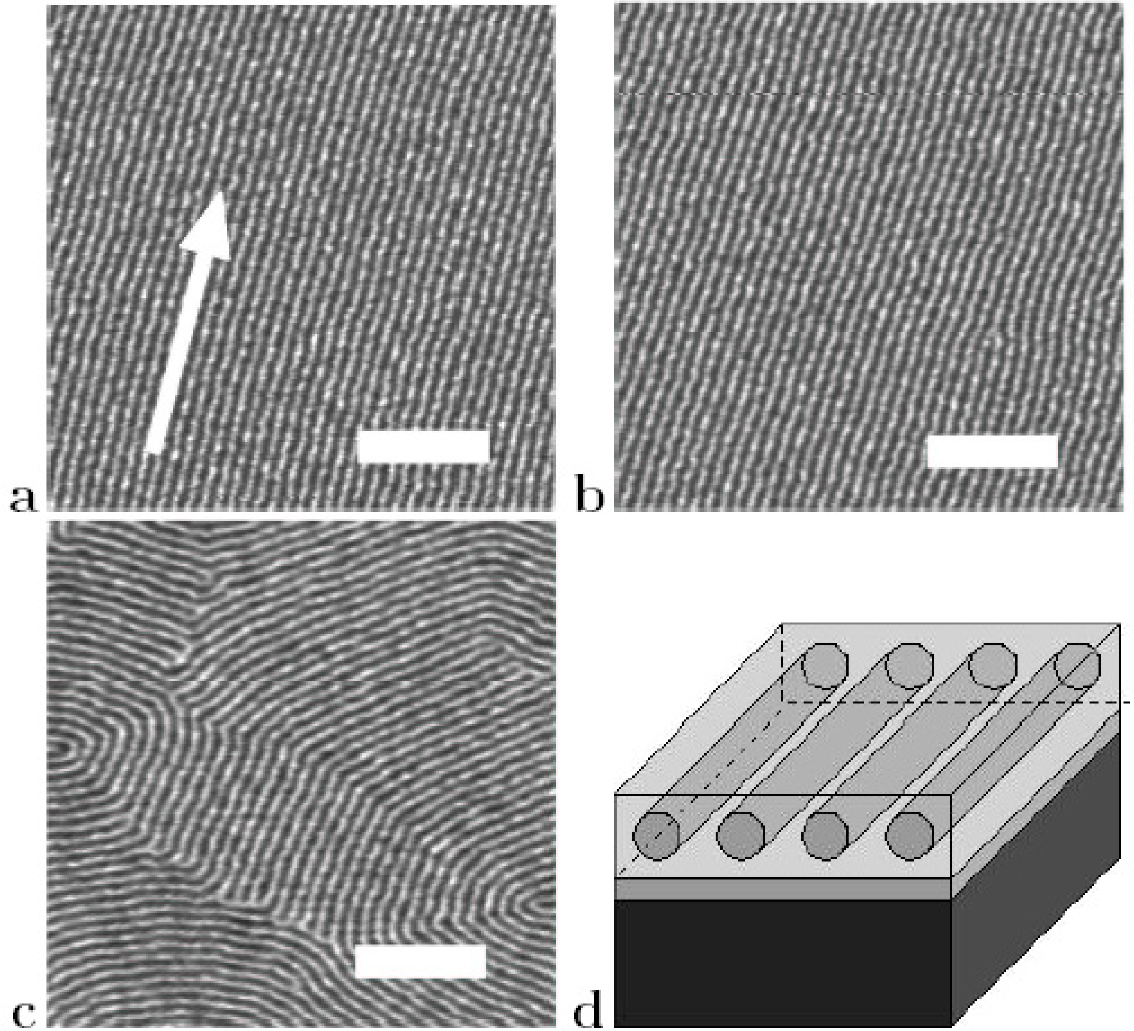

Figure 1: Panel a: An AFM micrograph acquired on a copolymer sample aligned by the method described in this paper. The cylindrical microdomains are in perfect registry, without any visible defect. The arrow indicates the shearing direction. Panel b: Another micrograph, acquired 8 mm away from the one shown in Panel a. A single dislocation is visible (these are particularly well aligned regions) Panel c: Fingerprint-like pattern characteristic of samples annealed without shearing. Scalebar = 250 nm. Panel d: Cartoon of a single layer of cylindrical microdomains. PS cylinders (darker gray) form within a matrix of PEP (lighter gray), with a PS wetting layer at the Si interface. Film thickness : 30 nm

Nano-rheometry

Polymer used : monolayer of cylinder-forming PS-PEP

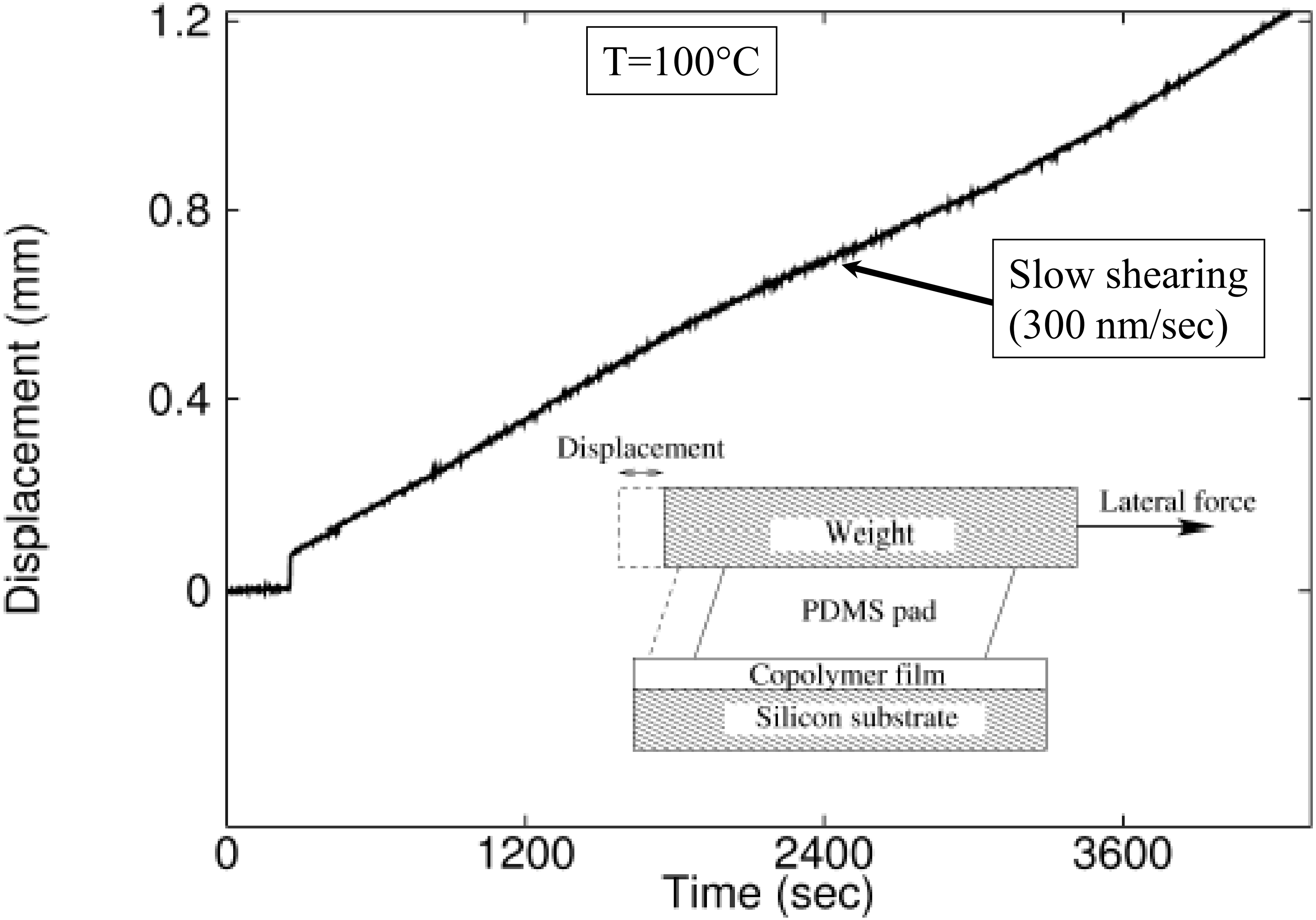

Thin film viscosity measurement

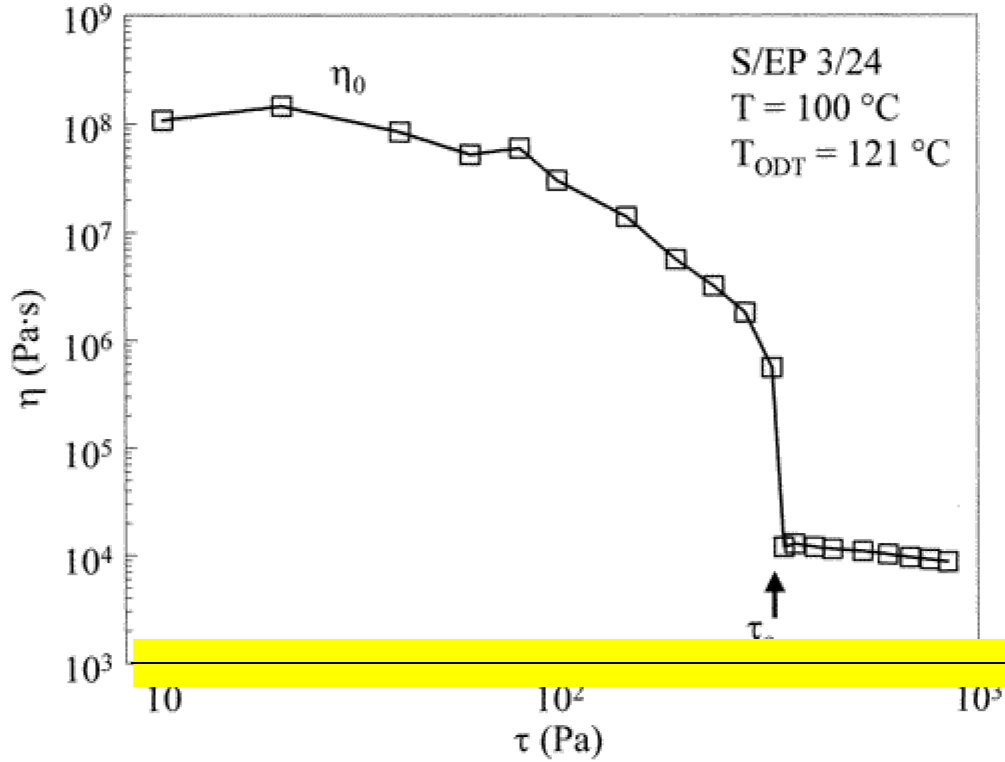

S/EP 3/24 Bulk Data

J Sebastian *et al*
Macromolecules **35** p. 2707-2713 (2002)

Cylinder and Sphere thin films

Applied stress

From the analysis of 2-layer cylinder and sphere data we get an apparent viscosity on the order of 1000 Pa s which is lower than expected for bulk.

We are in the stress regime where microdomain order is destroyed by shear !

Possible model

Assume misaligned cylinders rip off due to shear. Similar to an angle dependent Order-Disorer Temperature (TODT)

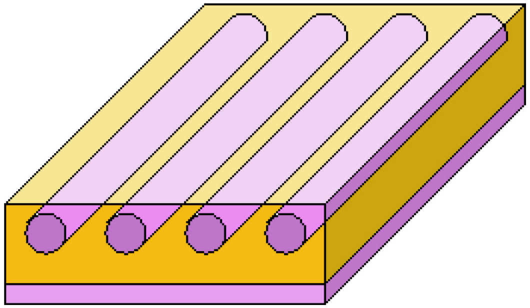

Cylinders “melt” due to shear

PDMS movement

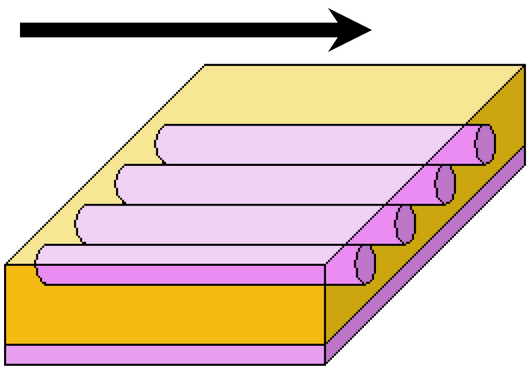

Cylinders are stable

$$T_{ODT}(\Theta) = T_{ODT}(1 - \dot{\gamma}\tau_{as}\sin^2(\Theta))$$

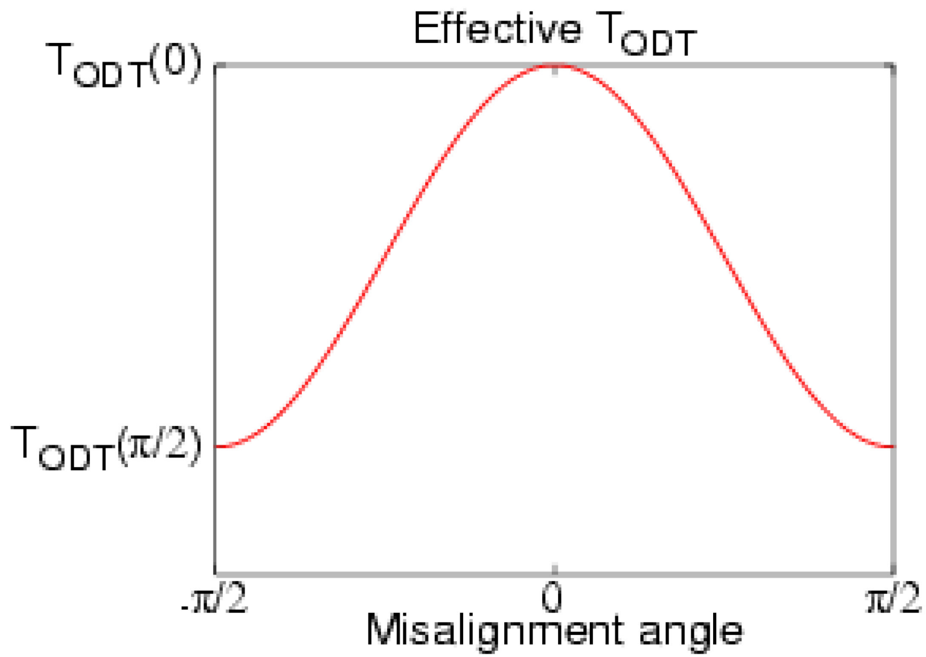

Cylinders will be “melted” unless the temperature is below the effective TODT. Thus, the will only be stable if they are within a narrow range of angles centered around the shearing direction. Otherwise they melt (or break) and reform.

Sphere Alignment : 2 Layers

(S/EP 3/24)

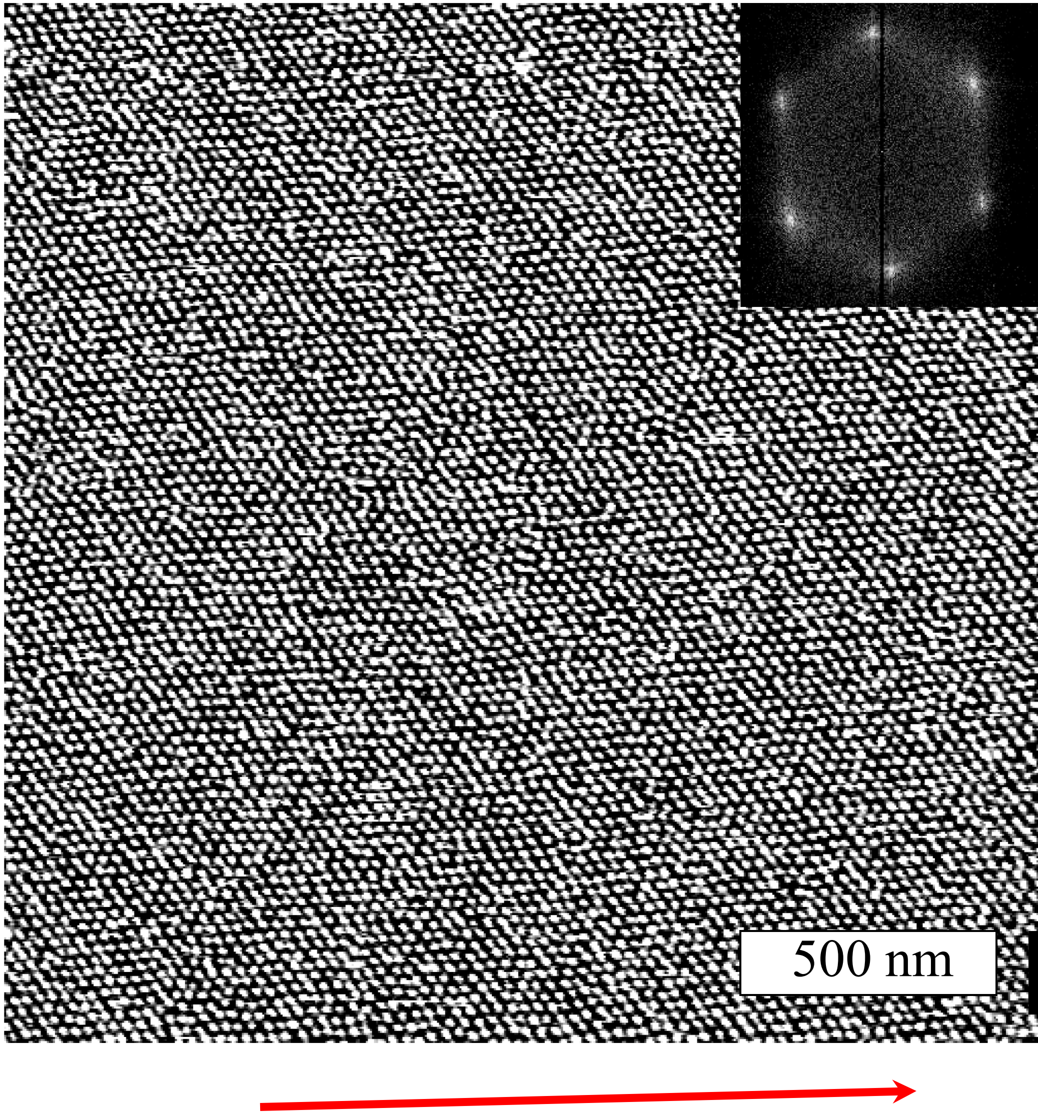

Spheres aligned over square cm !

- Only align if they are 2-layer thick.
- One lattice vector parallel to shearing direction (like colloids)
- Slip occurs at the interface between layers.

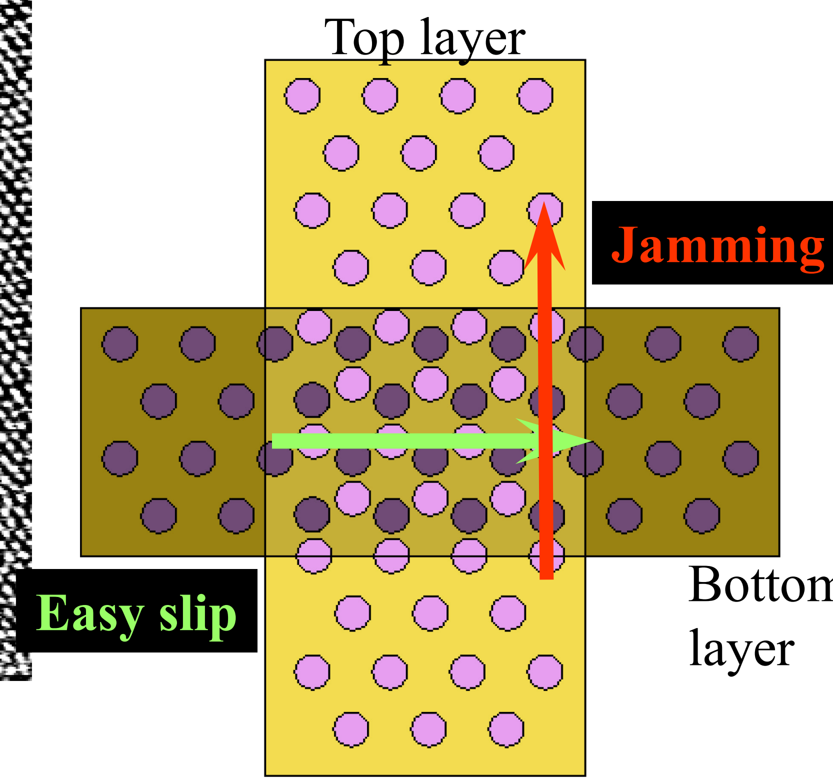

Shear Alignment of ***two*** layers of spheres

Complete alignment over cm,

No Disclinations, Greatly ***reduced*** dislocations

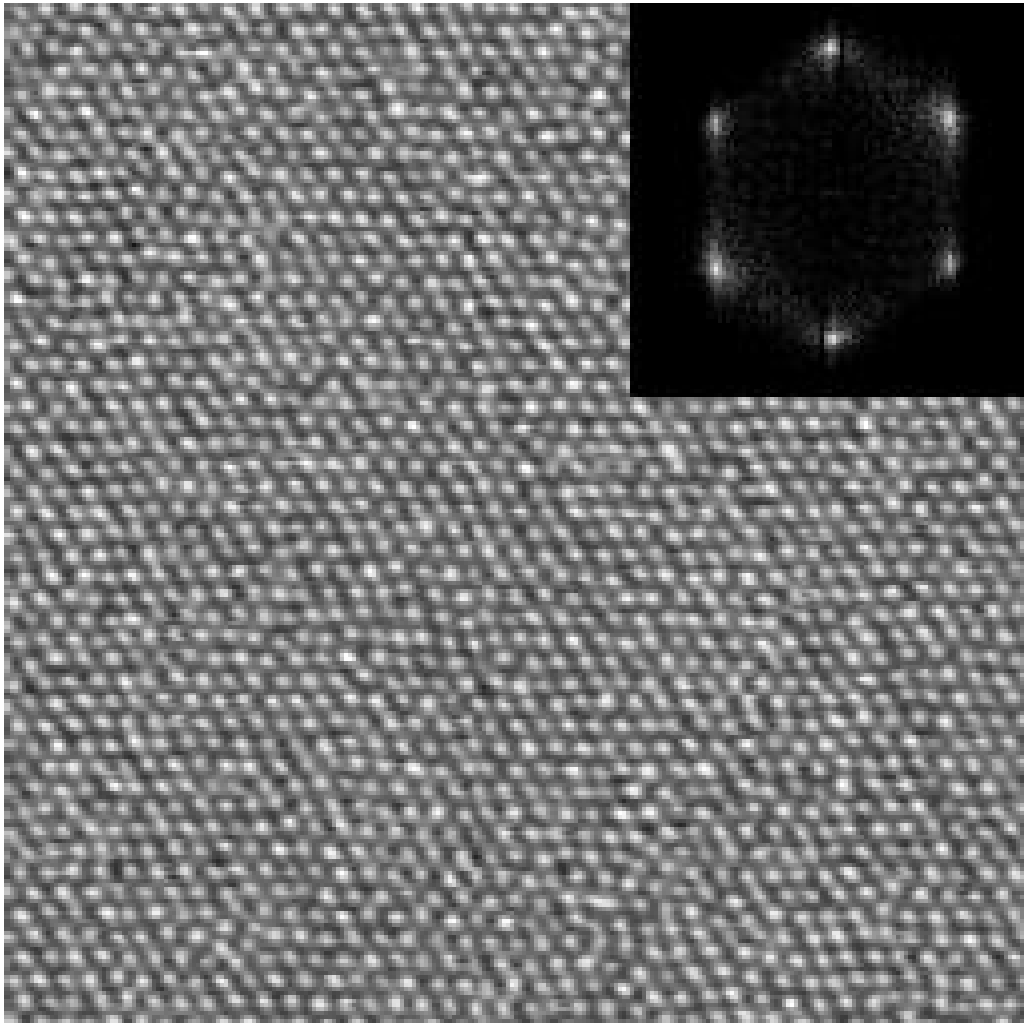

Transmitting Stress through a Fluid Layer

Rheometrics DSR-200
parallel plate fixtures
isometric view

cross-sectional
view

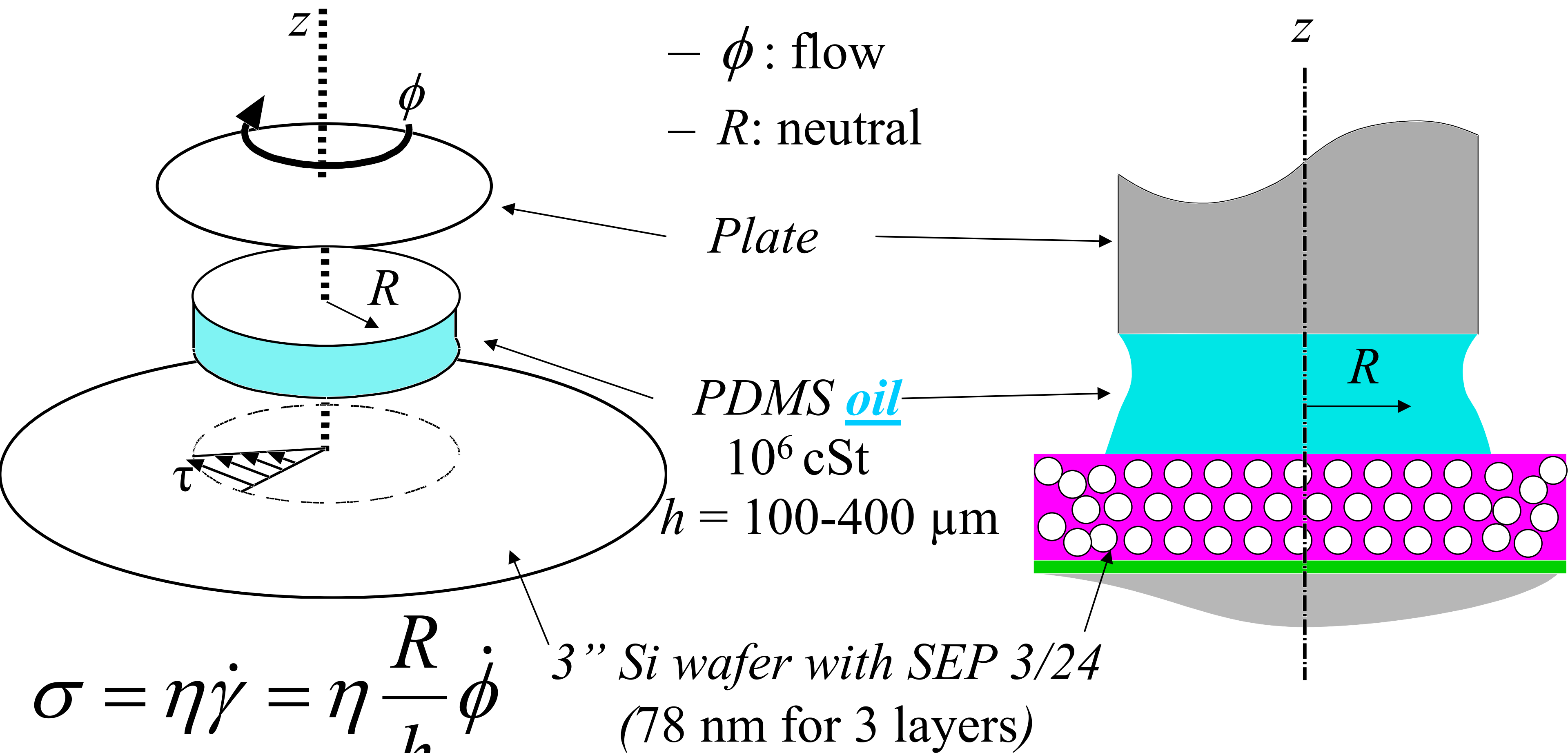

$$\sigma = \eta \dot{\gamma} = \eta \frac{R}{h} \dot{\phi}$$

Shearing – PS-PHMA 21-64

Shear annealed at 135°C for 30 minutes

$$S = \langle \cos(2\delta\theta) \rangle$$

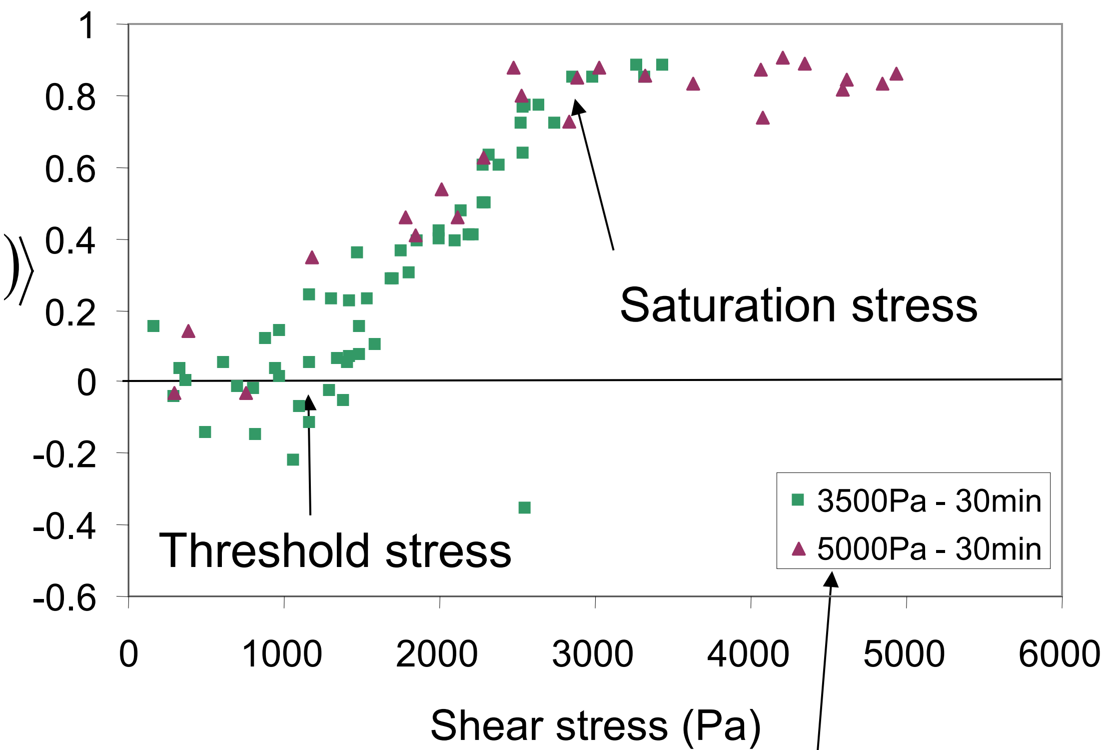

τ_{max} at edge

Sample is a quarter wafer

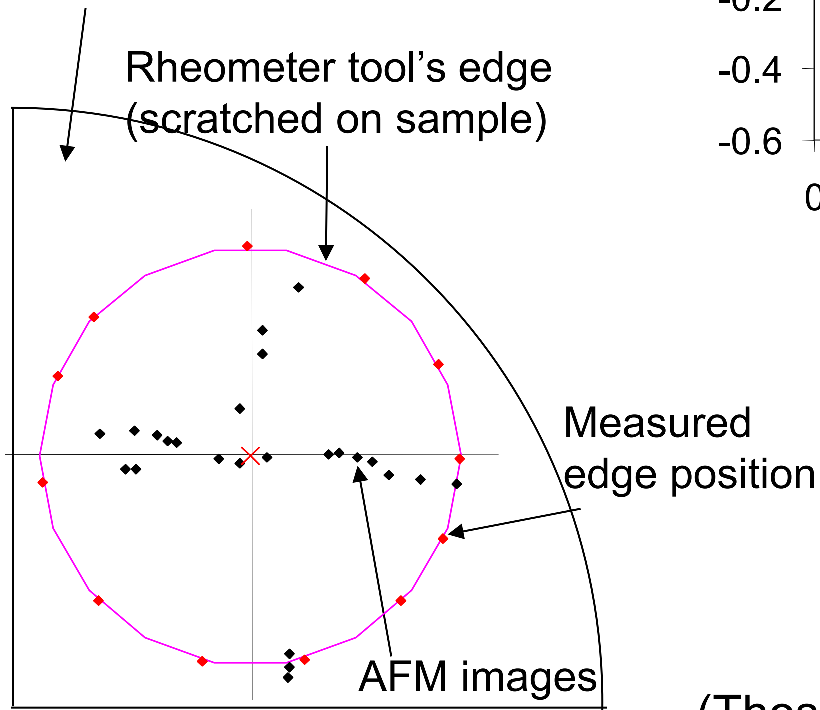

(Those are the triangles in the plot above)

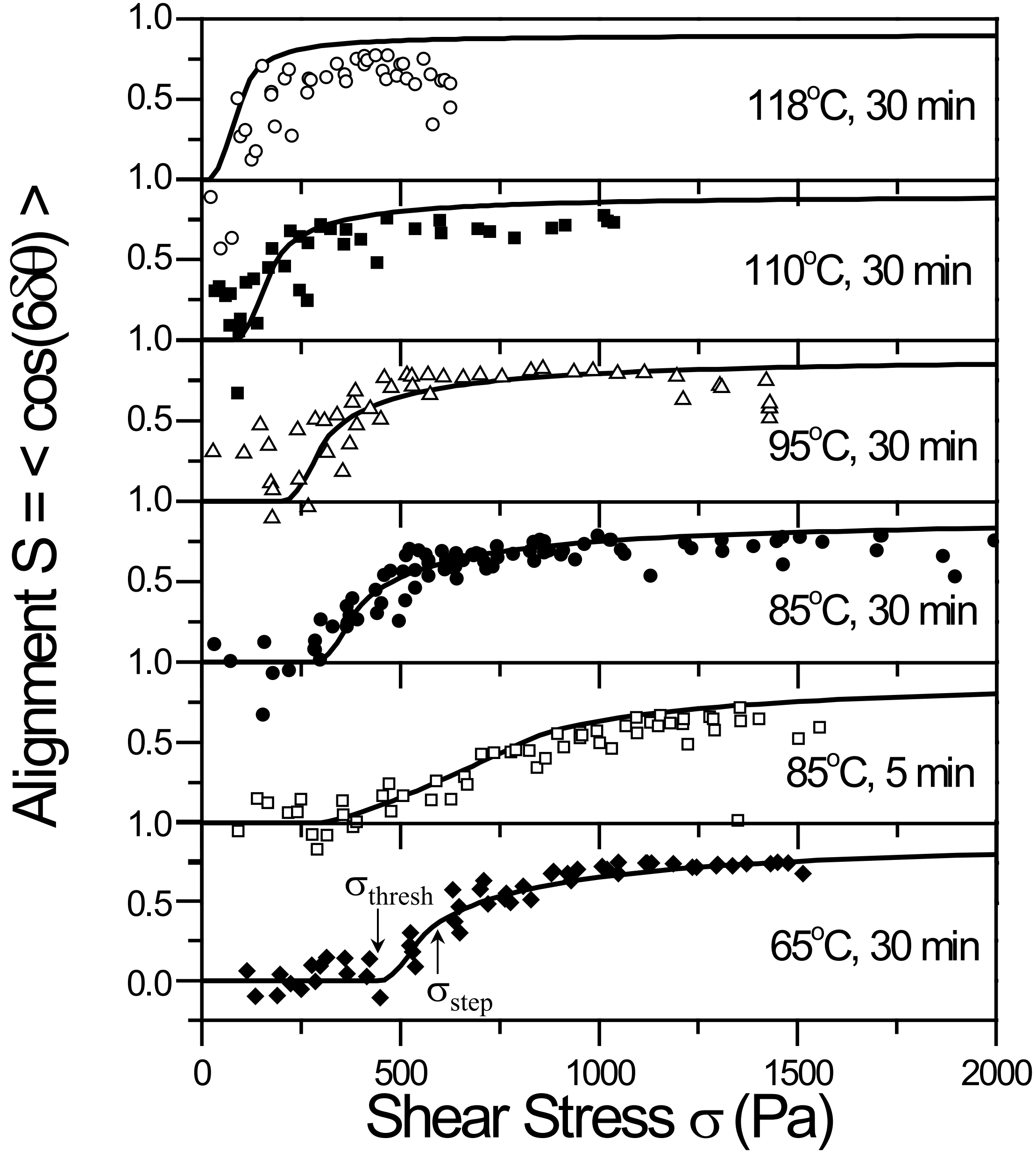

Alignment S = < cos(6δθ) >
Shear Stress σ (Pa)
118°C, 30 min
110°C, 30 min
95°C, 30 min
85°C, 30 min
85°C, 5 min
65°C, 30 min
σthresh
σstep
1.0
0.5
0.0
0
500
1000
1500
2000

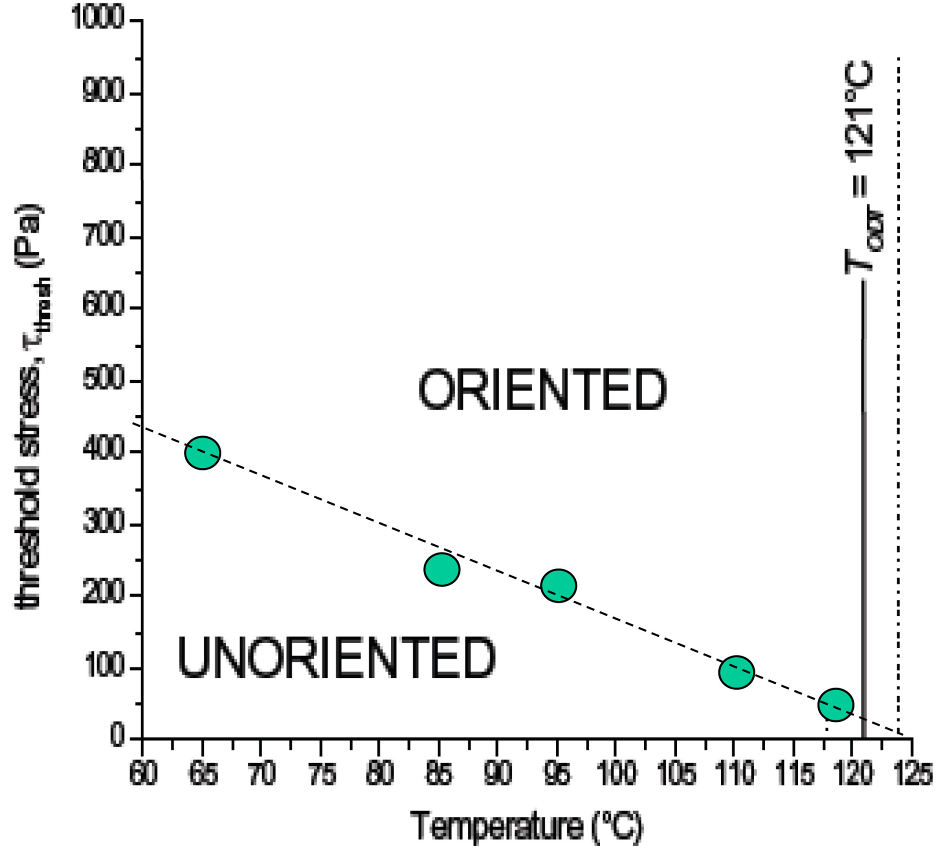

FIG. 5: Threshold stress as a function of temperature. The threshold stress line divides the aligned (above) and the less aligned and polygranular (below), while $T_{\rm ODT}$ and T_g (not shown) demarcate regions of disorder.

Recrystallization: T *vs.* T_{ODT}

Change in distribution

$$\Delta P(\theta) = \Delta t\ \Gamma(T_{\mathrm{ODT}}(\theta) - T) / T_{\mathrm{ODT}}$$

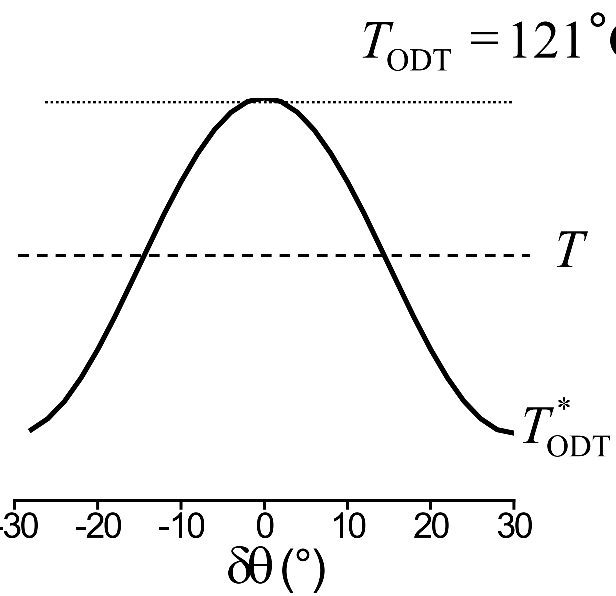

$$T_{\mathrm{ODT}}(\theta) = T_{ODT}(1 - (\sigma / \sigma_0)(\sin(3\delta\theta)^2)$$

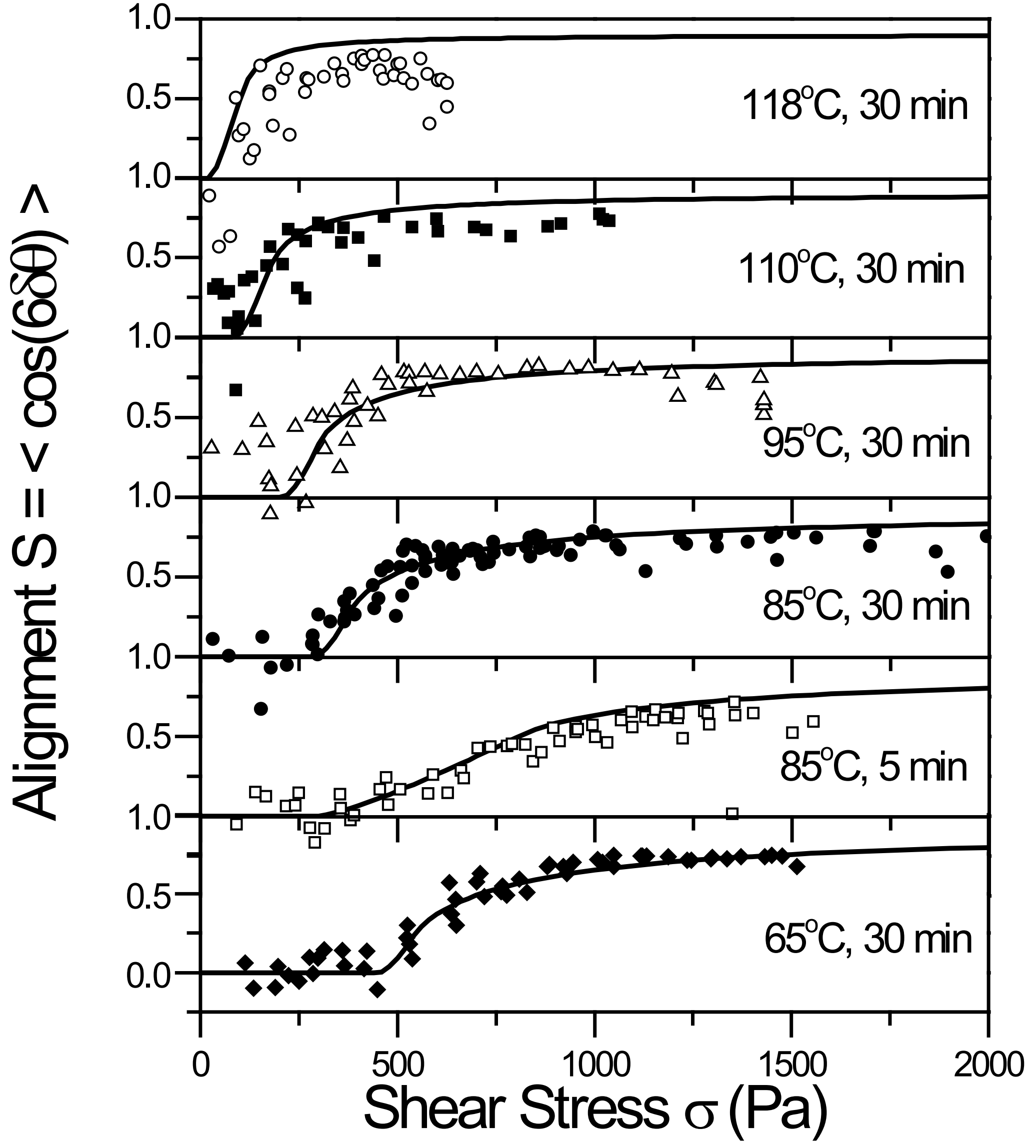

Free energy governing cell dynamics simulations

$$F[\psi(\mathbf{r})] = \int d\mathbf{r}\{\psi(\mathbf{r})[-\frac{\tau}{2} + \frac{a}{2}(1-2f)^2 - \frac{D}{2}\nabla^2 - \frac{D_x}{2}\partial_x^2]\psi(\mathbf{r}) +$$

$$+ \frac{\mu}{3}(1-2f)\psi(\mathbf{r})^3 + \frac{\lambda}{4}\psi(\mathbf{r})^4\} + \frac{c}{2}\int d\mathbf{r_1}\int d\mathbf{r_2} G(\mathbf{r_1}-\mathbf{r_2})\psi(\mathbf{r_1})\psi(\mathbf{r_2})$$

$$\frac{\partial\psi}{\partial t} = \nabla^2\frac{\delta F[\psi]}{\delta\psi} + \xi$$

Shear rate $\dot{\gamma}$

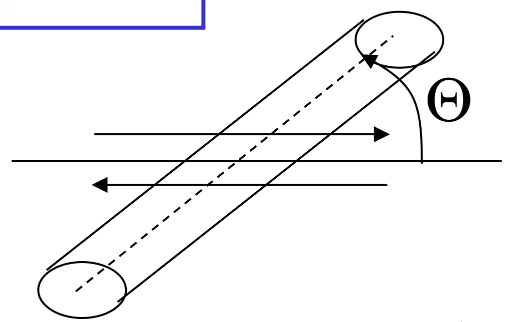

$$D_x \propto \dot{\gamma}\tau_{as}\sin^2(\Theta)$$

Time to destroy by shear = $\frac{1}{\dot{\gamma}\sin(\Theta)}$

Assembly time τ_{as}

Adapted from I. Hamley *Macromol. Theory Simul.* **9**, 363 (2000)

Two Square Layers, Interacting

ψ_1

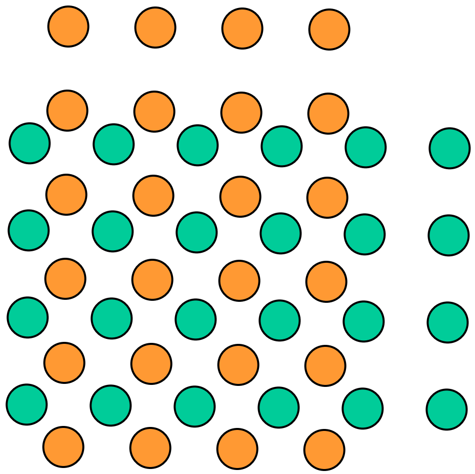

ψ_2

$\psi_i = \delta\rho_i[\cos(2\pi(x_i - x_{i,0)})+\cos(2\pi(y_i - y_{i,0}))]$

is the order parameter for a square density wave

$$F = a(T - T_{ODT})\psi_1^2 + u\psi_1^4 + a(T - T_{ODT})\psi_2^2 + u\psi_2^4 + \Gamma\psi_1\psi_2$$

$$F = a'(T - T_{ODT})\psi^2 + u'\psi^4 + \Gamma\psi^2 = a'(T - T_{ODT}^*)\psi^2 + u'\psi^4$$

$$T^*_{ODT} = T_{ODT} - \Gamma / a'$$

where a’=2a, u’=2u

Shear at an angle to lattice

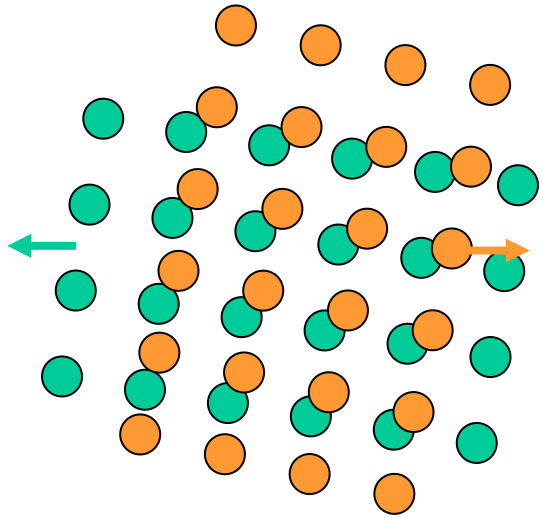

Now comes the real fudge, time average over relaxation time

$$\Gamma \propto \dot{\gamma}\tau \sin^2(3\theta) \sim \frac{\sigma}{\sigma_0}\sin^2(3\delta\theta)$$

$$T_{\mathrm{ODT}}(\theta) = T_{ODT}[1-(\sigma/\sigma_c)\sin^2(3\delta\theta)]$$

Channel Flow – Motivation

Since we can **transmit** the shear stress using PDMS oil, we should be able to **produce** it with **pressurized flow**.

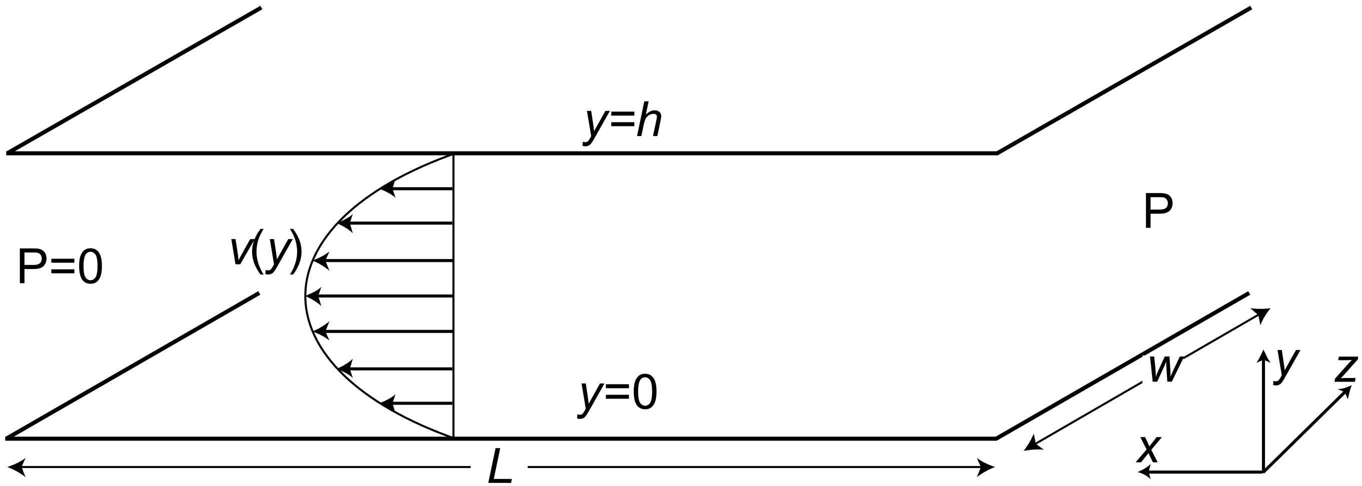

$$\left(\frac{\partial^2}{\partial y^2}+\frac{\partial^2}{\partial z^2}\right)v_x(y,z)=\frac{\Delta P}{\eta L}$$

$$\tau=\eta\left.\frac{\partial v}{\partial y}\right|_{wall}$$

Channel Flow – Setup

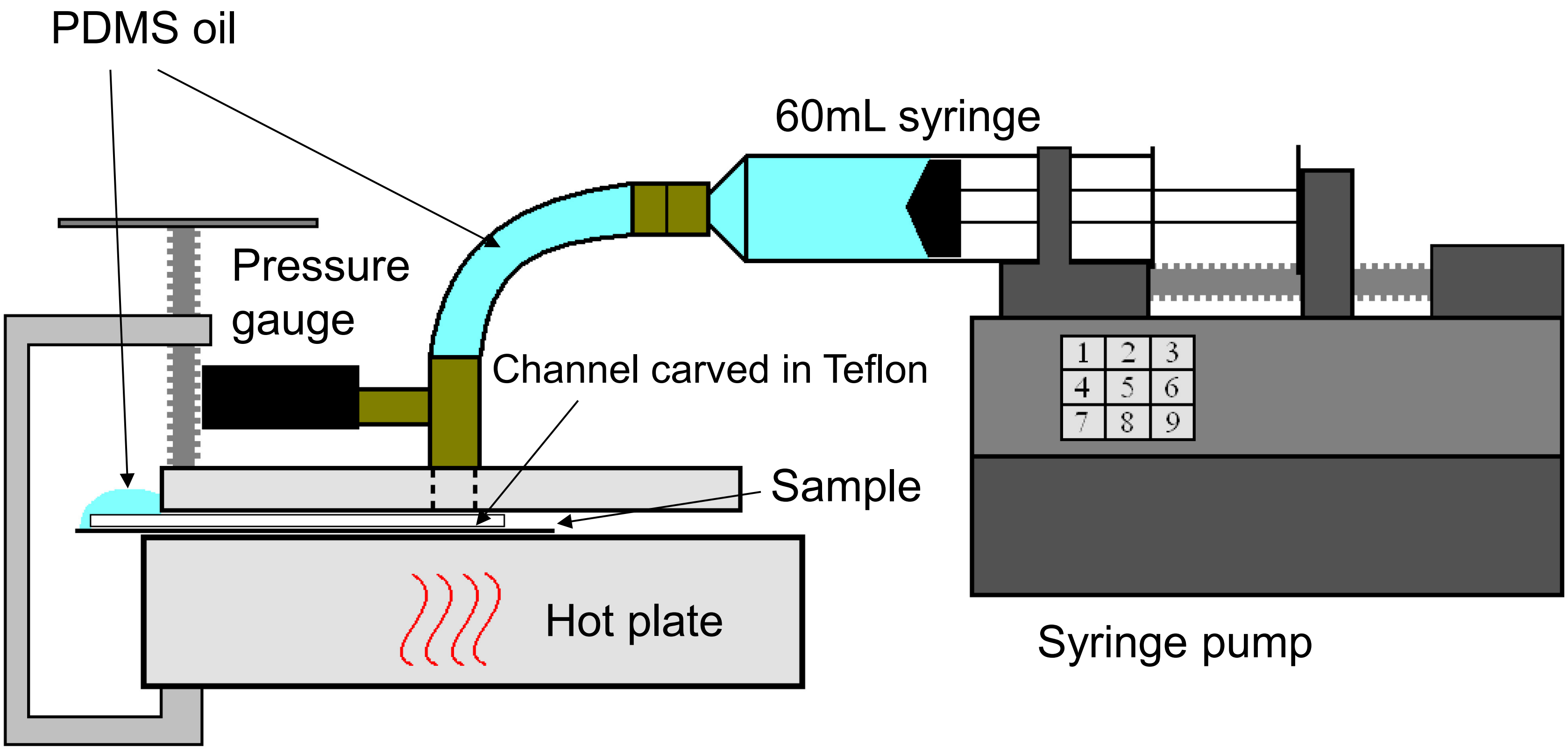

Channel Flow – VIN Channel

PS-PEP 5-13
120°C
600Pa

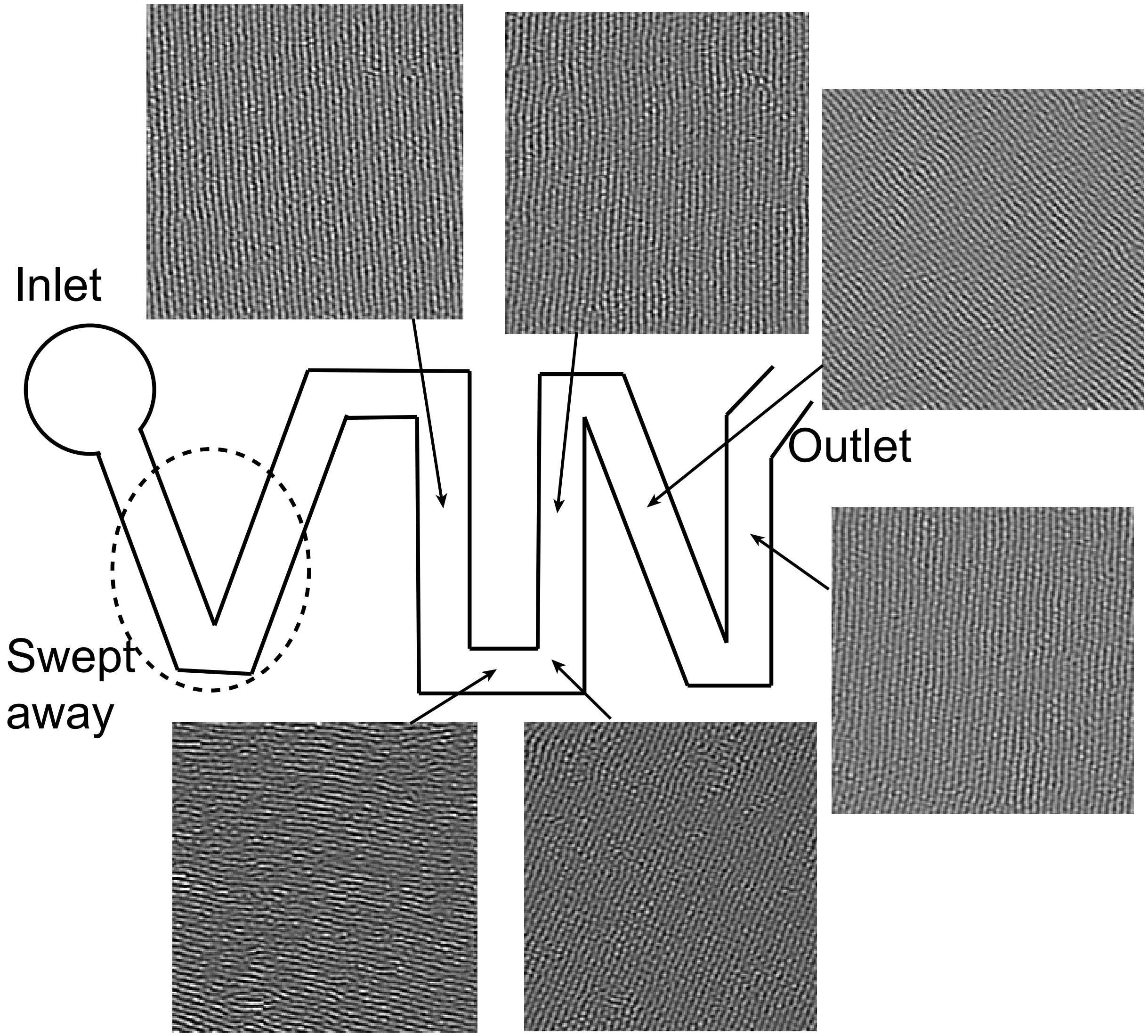

Channel Flow – Double Wedge

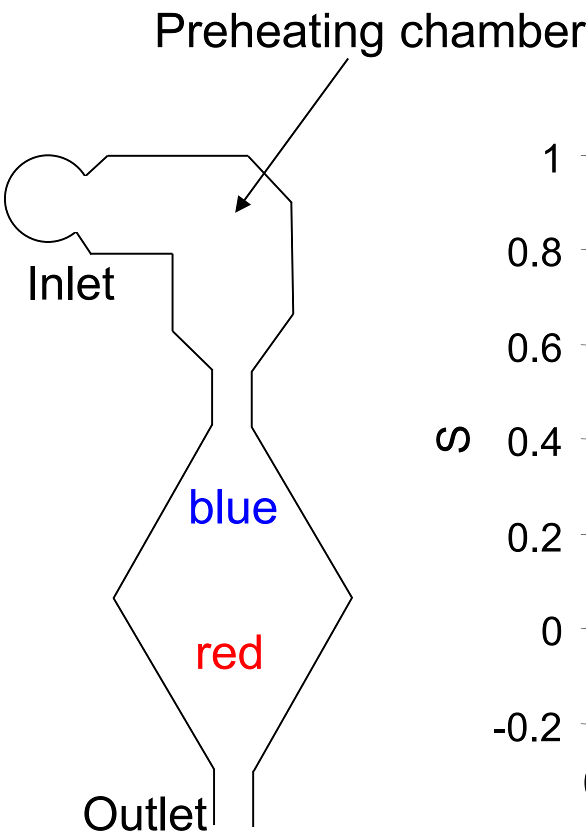

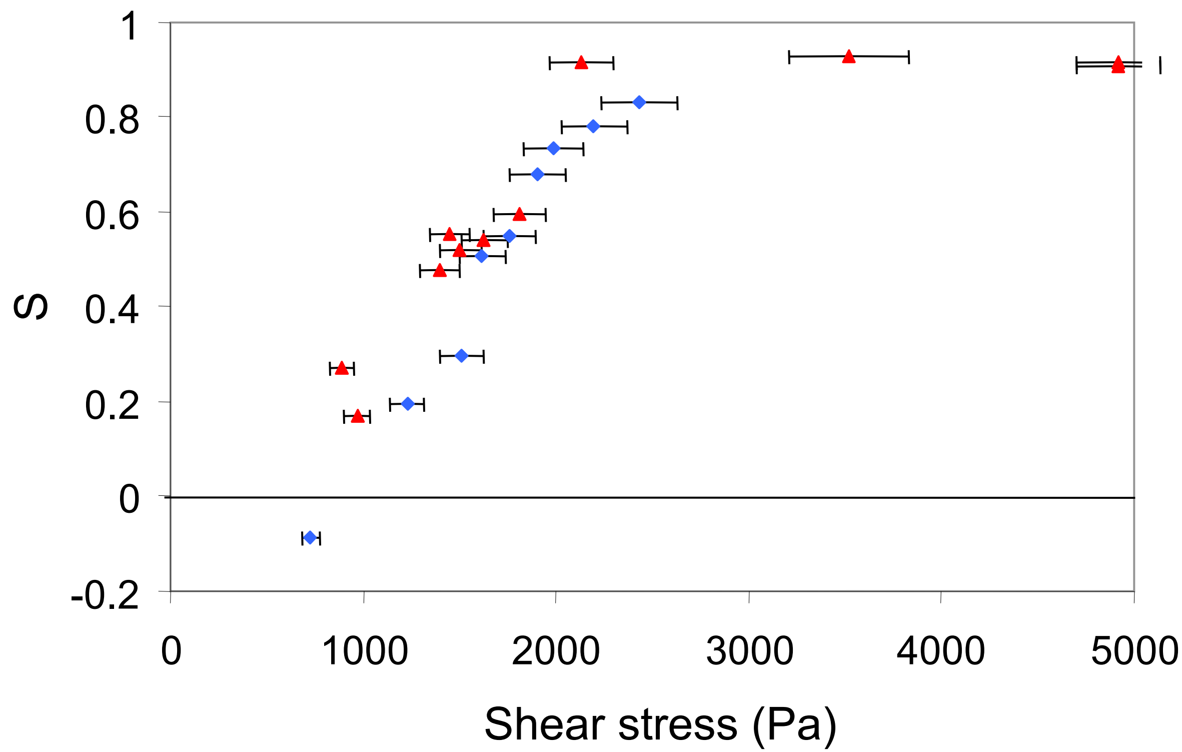

Get stress from flow rate and local channel width.

Model – PS-PHMA

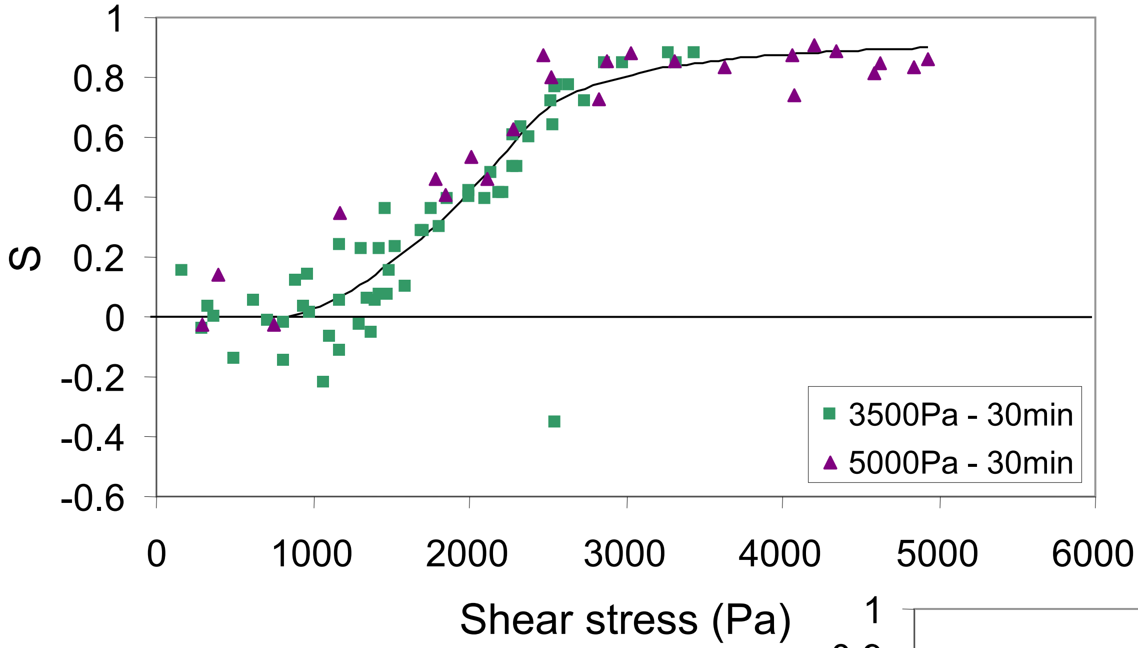

PS-PHMA 21-64

PS-PHMA 30-84

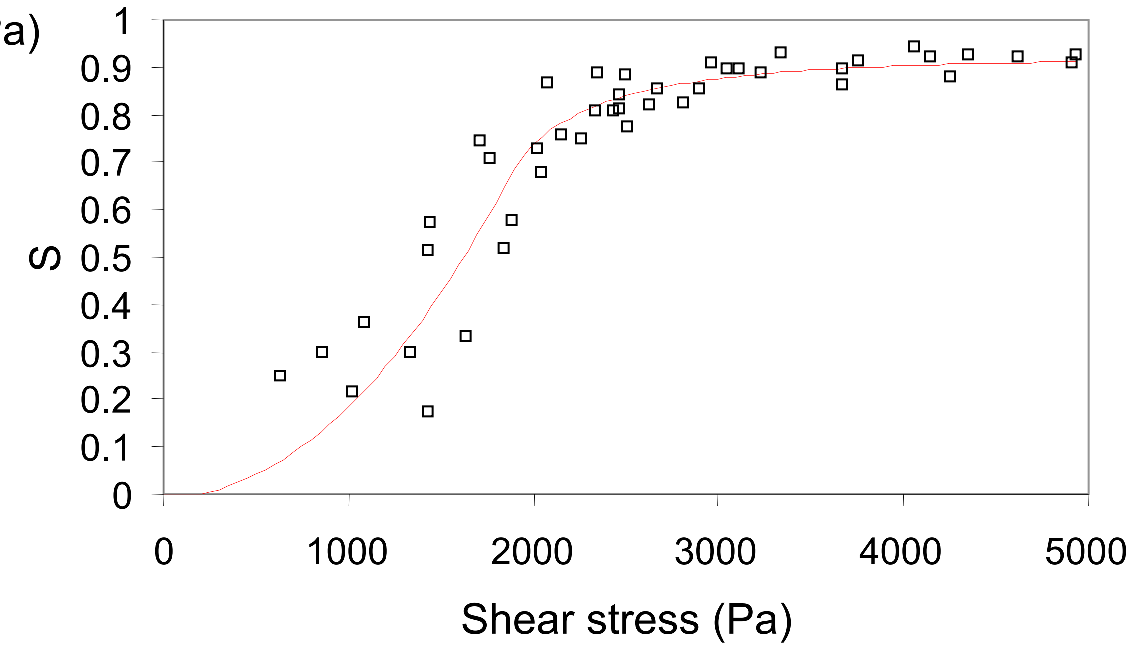

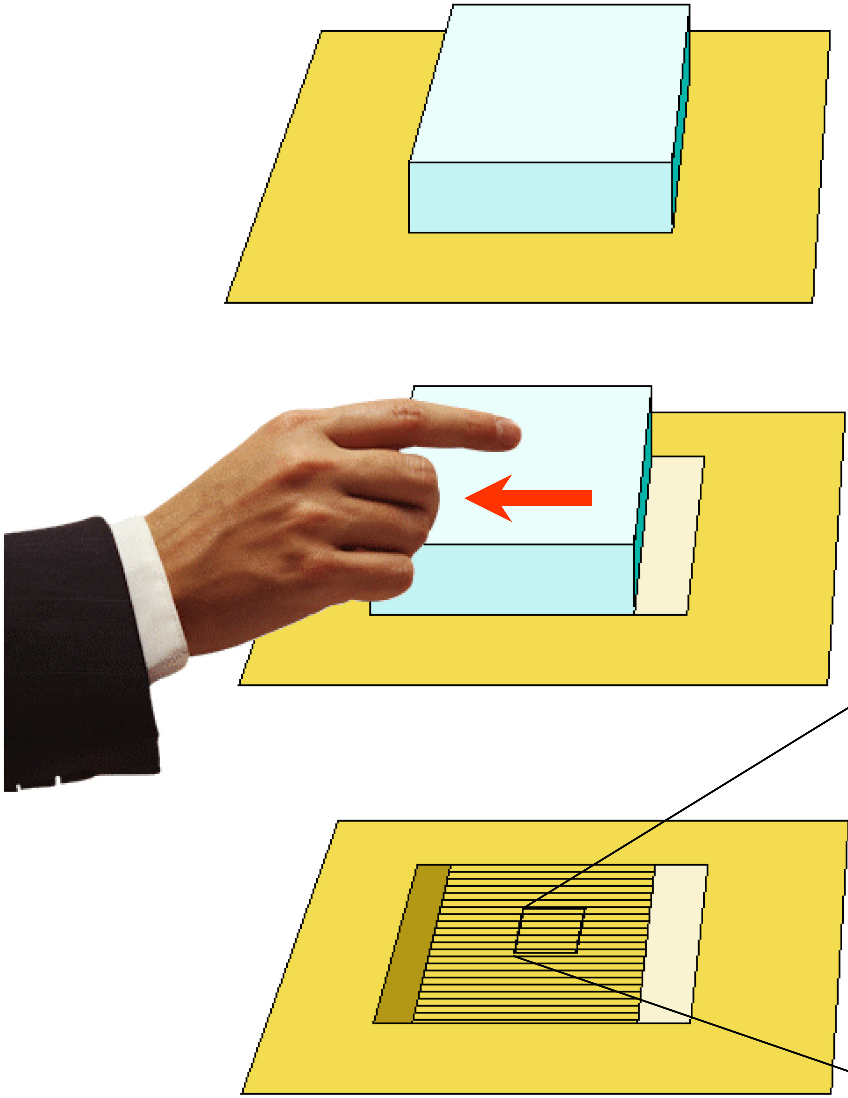

• easy alignment method over square cm for both cylinders and spheres

• system for studying the mechanisms responsible for shear alignment

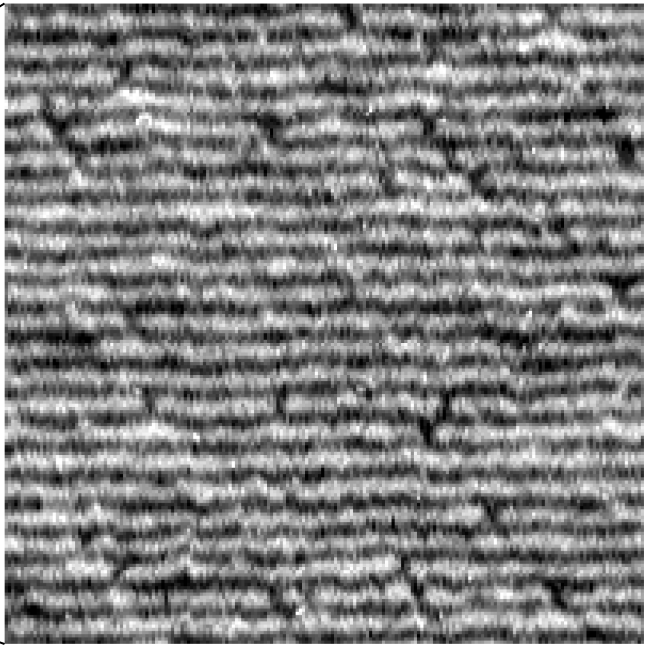

PS-PHMA film

Characteristic correlation lengths (30nm period):

As cast	100nm
1 hr. anneal	1μm
Anneal limit	5μm
Zone Refine	50μm
Shear align	>2cm

Polarizers – SEMs

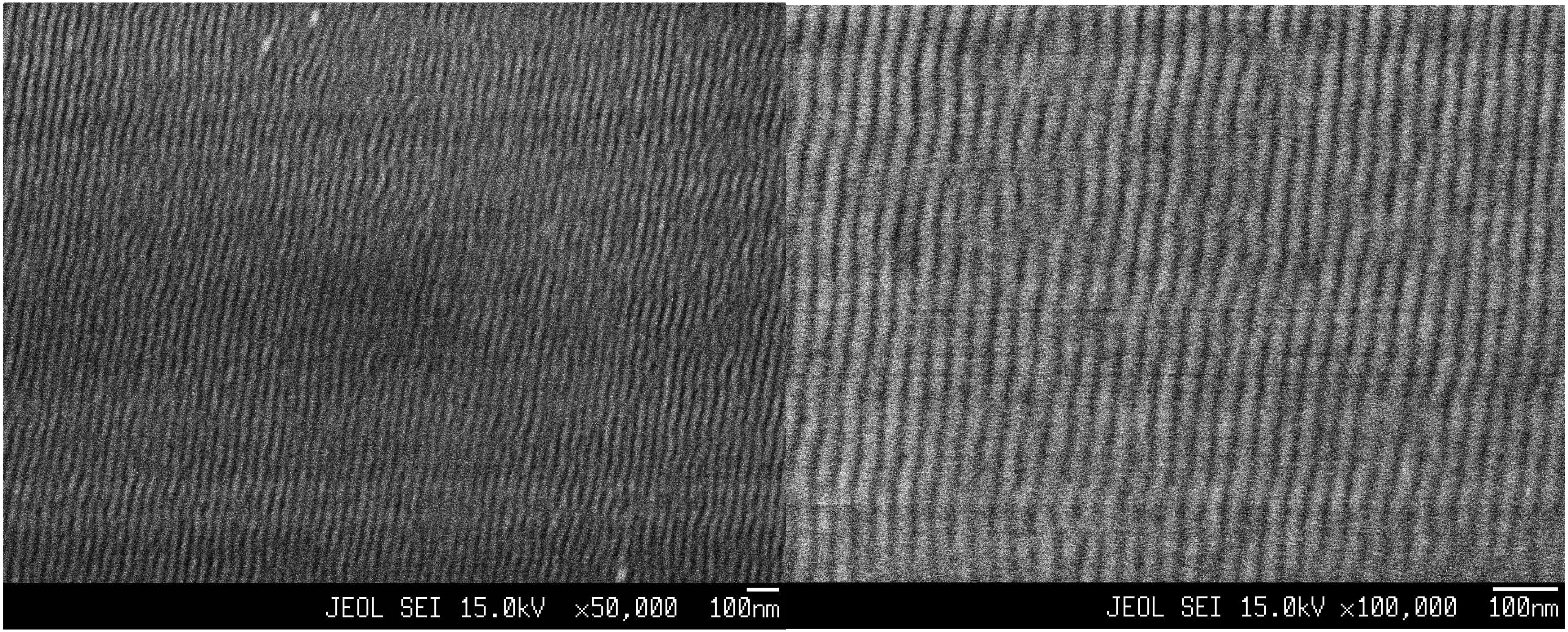

SEM of a sample with aluminum wires on a Si wafer.

Quantitative Measurements of Polarization

- use laboratory UV-vis spectrometer (in air)
- put two nanowire polarizers in train, measure transmitted intensity with wires parallel and crossed

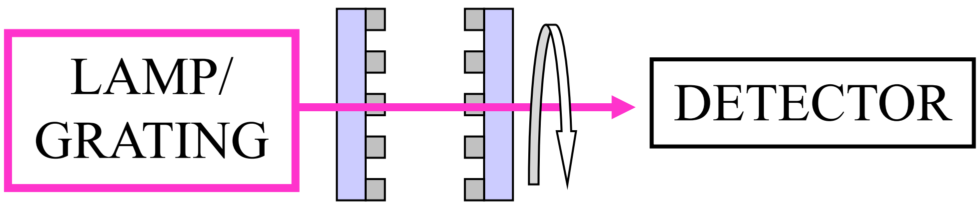

$$\mathrm{POL} = \left(\frac{\parallel - \perp}{\parallel + \perp} \right)^{1/2}$$

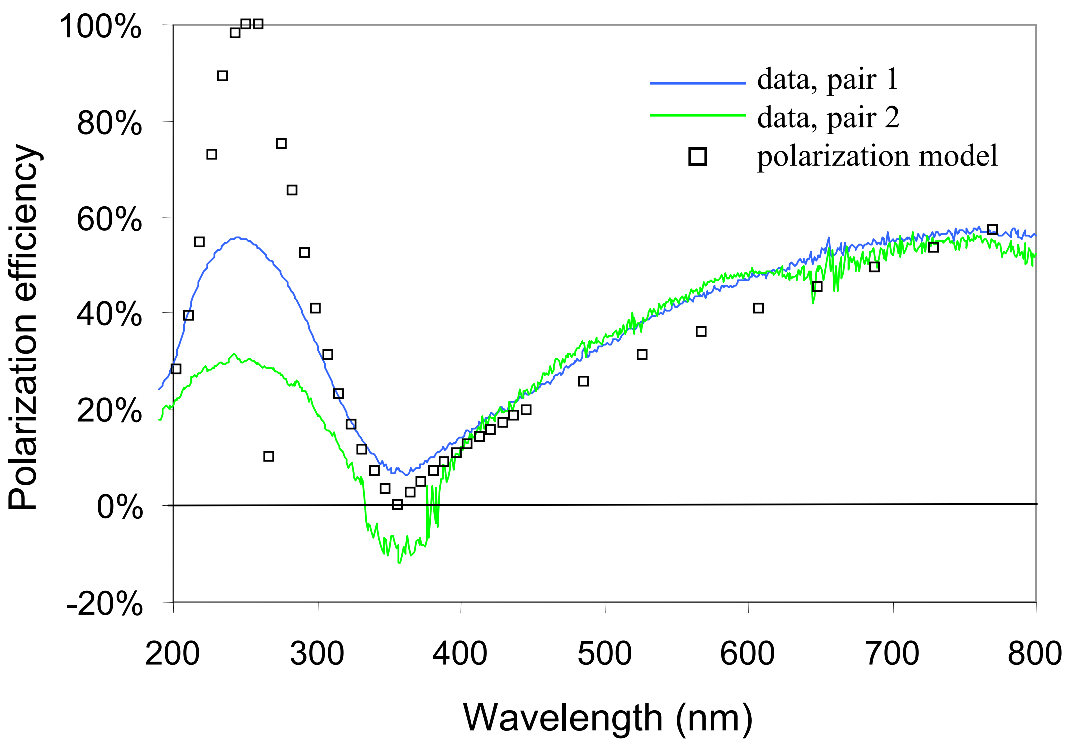

- POL ≈ 30% in the visible, goes to zero near 350 nm
- for wavelengths below the node (closer to the metal's plasma frequency), light polarized *transverse* to the wires is preferentially transmitted

Polarizers – UV Crystal Analyzer

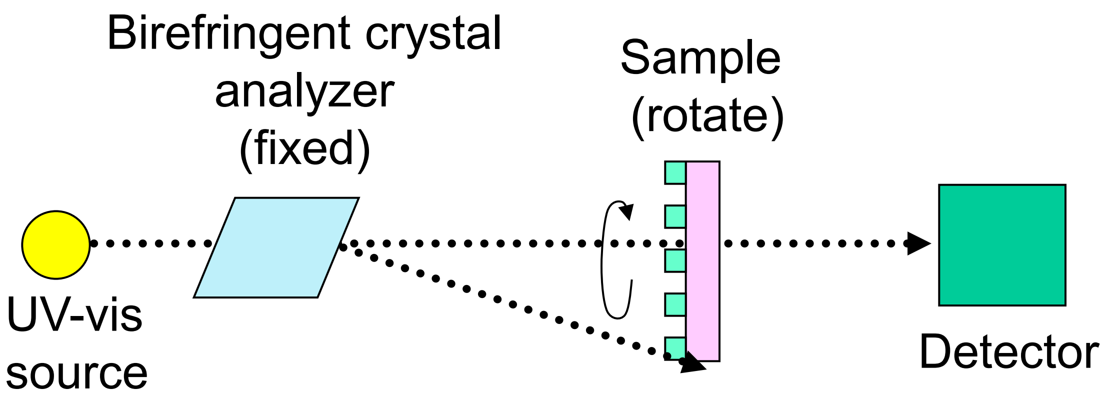

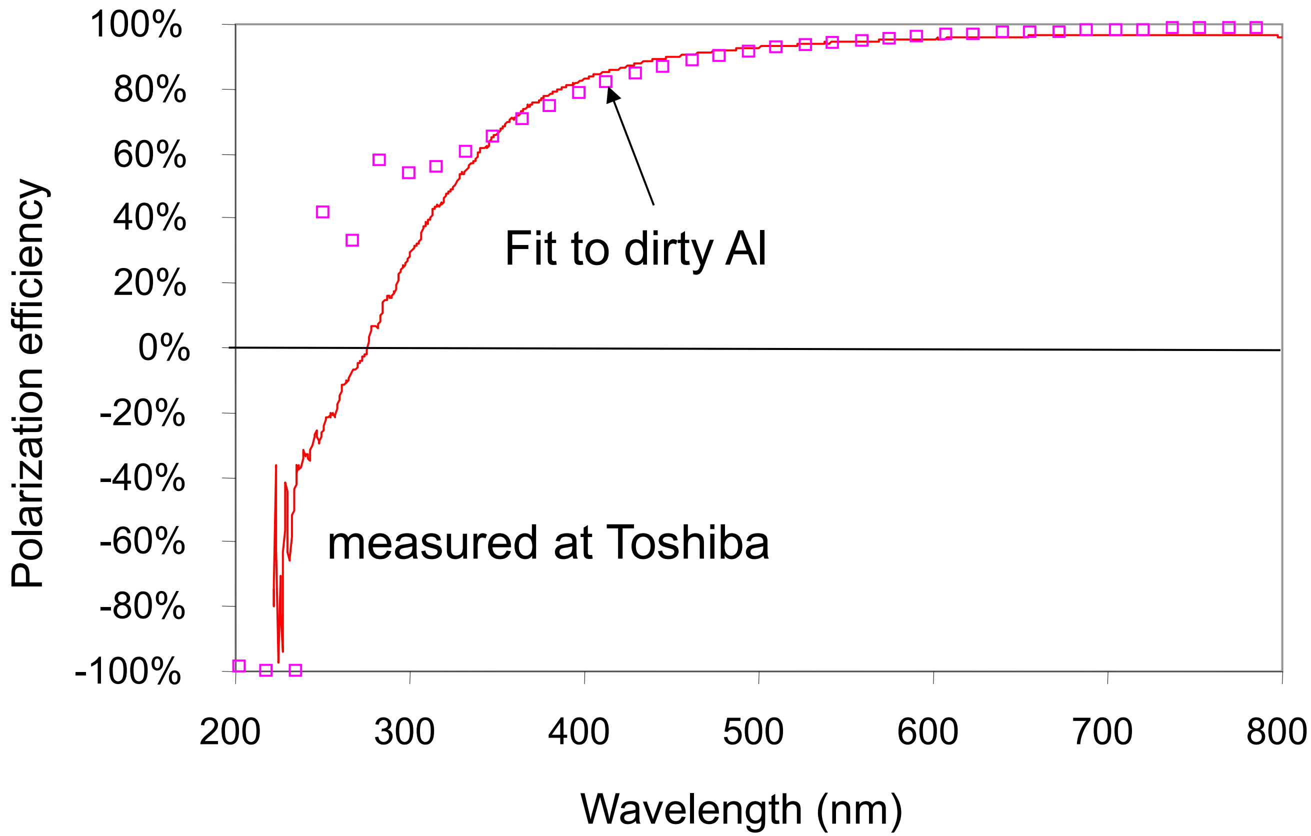

Polarizers – The Movie

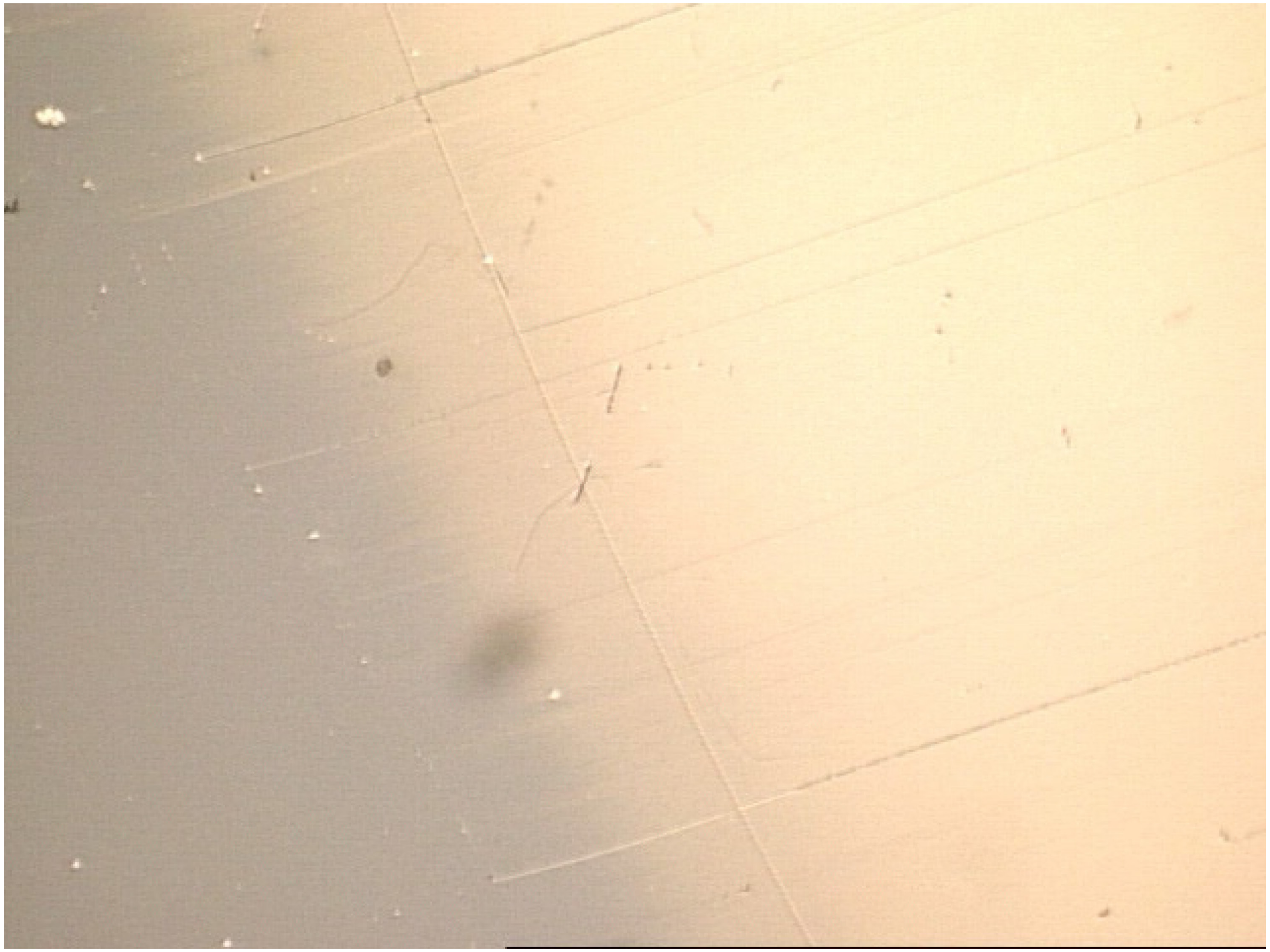

This is one of the samples, as viewed in an optical microscope with a polarizer analyzer. The field of view is 2.1mm by 1.6mm.

This is the edge of the shear-aligned region.

IBM Nanotechnology announcement at IEDM

IBM used self assembly to build a nanocrystal FLASH memory device

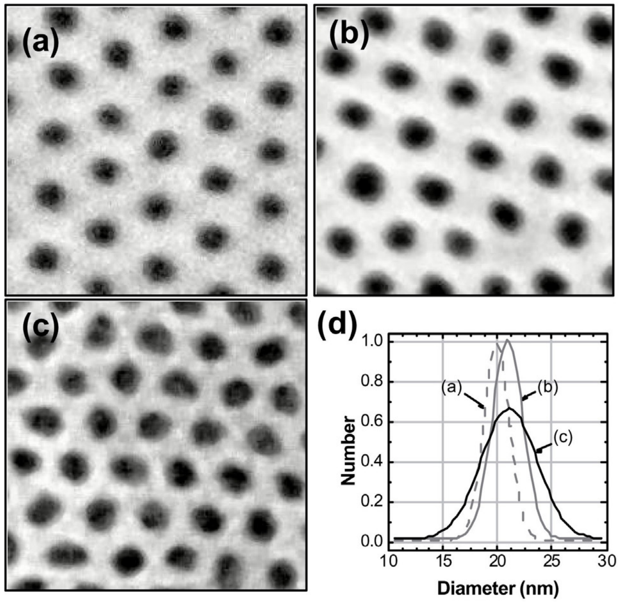

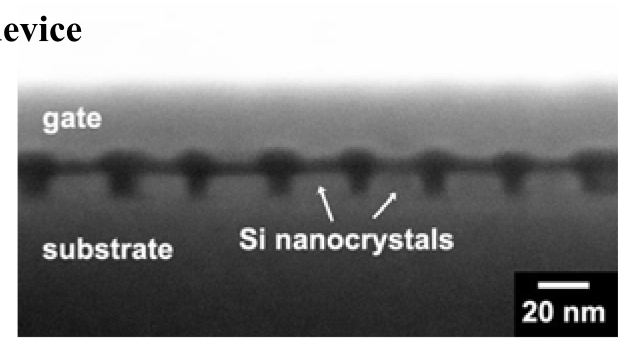

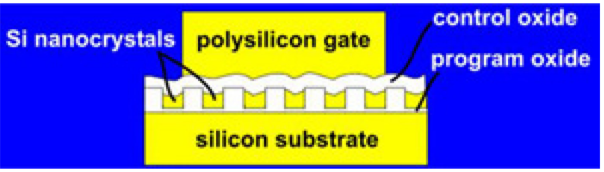

Toshiba

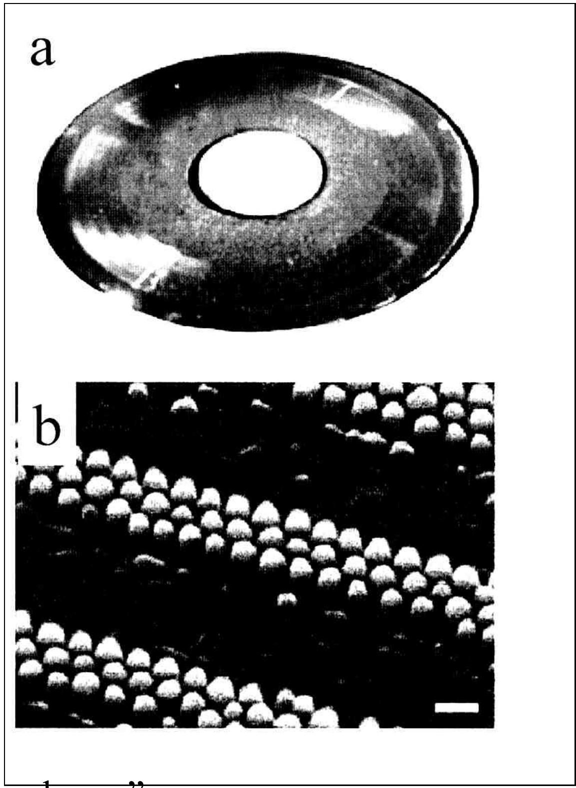

SEM image of the patterned magnetic media with a 40 nm diameter. The scale bar indicates 100nm.

"Nano-Patterning for Patterned Media using Block-Copolymer", Koji Asakawa, Toshito Hitaoka, Hiroyuki Hieda, Masatoshi Sakurai, Yoshiyuki Kamata and Katsyuki Naito., J. Photopolymer Science and Technology Vol.15, p. 465 (2002)

Conclusions

- Nanolithography with Diblock Copolymers ***WORKS***
  - 5-50 nm patterns, $10^{11} – 10^{12}$ /cm^2
  - Wide variety of substrates and transfers
  - Standard Semiconducting Processing

- Ordering Kinetics
  - $T^{1/4}$ in both stripes and hexagons
  - Quadrupole annihilation in stripes!
  - Disclinations again in hexagonal

- Shear Alignment gives long range order
  - Cylinders work in a monolayer, better in 2 layers
  - Spheres work in two or more layers
  - Melting/Recrystallization model with $T^*_{ODT}(\theta)$ describes results well ???

- Alignment with channel flow, can pattern stripes